J. Fluid Mech. (1994), *vol.* 275, *pp.* 1–32

Experiments on a round turbulent buoyant plume

By AAMIR SHABBIR† AND WILLIAM K. GEORGE

Department of Mechanical and Aerospace Engineering, State University of New York at Buffalo, Buffalo, NY 14260, USA

(Received 8 January 1990 and in revised form 11 February 1994)

This paper reports a comprehensive set of hot-wire measurements of a round buoyant plume which was generated by forcing a jet of hot air vertically up into a quiescent environment. The boundary conditions of the experiment were measured, and are documented in the present paper in an attempt to sort out the contradictory mean flow results from the earlier studies. The ambient temperature was monitored to ensure that the facility was not stratified and that the experiment was conducted in a neutral environment. The axisymmetry of the flow was checked by using a planar array of sixteen thermocouples and the mean temperature measurements from these are used to supplement the hot-wire measurements. The source flow conditions were measured to ascertain the rate at which the buoyancy was added to the flow. The measurements conserve buoyancy within 10%. The results are used to determine balances of the mean energy and momentum differential equations. In the mean energy equation it is found that the vertical advection of energy is primarily balanced by the radial turbulent transport. In the mean momentum equation the vertical advection of momentum and the buoyancy force balance the radial turbulent transport. The buoyancy force is the second largest term in this balance and is responsible for the wider (and higher) velocity profiles in plumes as compared to jets. Budgets of the temperature variance and turbulent kinetic energy are also determined in which thermal and mechanical dissipation rates are obtained as the closing terms. Similarities and differences between the two balances are discussed. It is found that even though the direct effect of buoyancy in turbulence, as evidenced by the buoyancy production term, is substantial, most of the turbulence is produced by shear. This is in contrast to the mean velocity field where the effect of the buoyancy force is quite strong. Therefore, it is concluded that in a buoyant plume the primary effect of buoyancy on turbulence is indirect, and enters through the mean velocity field (giving larger shear production).

1. Preliminaries

1.1. *Introduction*

Buoyancy plays an important role in a number of fluid flows of environmental and technological importance. Examples include vertical motion of air in the atmosphere, spreading of smoke and other pollutants in the atmosphere, dispersal of volcano exhaust and water outfalls, and numerous industrial problems involving the natural-convection cooling of isolated sources. The buoyancy force in such flows can either be caused by a heat source, as in a smoke stack, or it can be caused by the introduction of one fluid into another fluid of different density, as in a water outfall. Once the fluid

† Present address: Center for Modeling of Turbulence and Transition, Institute for Computational Mechanics in Propulsion, NASA Lewis Research Center, Cleveland, OH 44135, USA.

is set into motion, its velocity field affects the thermal field, and vice versa. The initial state of laminar motion very quickly changes into turbulence and the flow starts to spread radially by entraining ambient fluid into the main flow. The laboratory plume is an idealization of these naturally occurring flows and it allows us to study the influence of buoyancy on turbulence. It can be shown that regardless of the kind of source, all plumes are dynamically similar as long as the density differences between the flow and the ambient surroundings are small compared to some reference density in the flow. Therefore, for convenience, and with no loss of generality, the source of buoyancy in this paper will be assumed to be heat and the density differences will be characterized by the temperature differences.

In the analysis of such flows the ambient fluid is assumed to be at rest. If its temperature does not change with height, the environment is termed as neutral. If the ambient temperature increases with height the environment is called unstable, and provides an additional source of buoyancy force. In a stable environment the temperature decreases with height and the growth of the plume is suppressed. This paper reports hot-wire measurements of a round turbulent buoyant plume in a neutral environment.

1.2. *Historical development*

The plume has been the subject of study since the similarity analysis of Zel'dovich (1937). Schmidt (1941) used mixing-length-type hypotheses to obtain expressions for the mean velocity and temperature profiles for both plane and round geometries and compared the results with his own measurements. Batchelor (1954) proposed similarity solutions for turbulent plumes for both plane and round geometries in neutral and stratified environments. For the round plume in a neutral environment, the mean vertical velocity and effective buoyancy acceleration were shown to be given by

$$W = F_0^{1/3} z^{-1/3} f_W(r/z), \tag{1}$$

$$g\frac{\Delta\rho}{\rho_\infty} = F_0^{2/3} z^{-5/3} f_T(r/z), \tag{2}$$

where F_0 is the rate at which buoyancy is added at the source, z is the height, r is the radial distance, g is the gravitational acceleration, ρ_∞ is the reference density (usually at infinity) and $\Delta\rho$ is the difference between the reference and the local mean density. The similarity variable is $\eta = r/x$ and the functions f_W and f_T are to be determined from experiments. It is common to represent these by Gaussian functions of the form

$$f_W(\eta) = A_W \mathrm{e}^{-B_W \eta^2}, \tag{3}$$

$$f_T(\eta) = A_T \mathrm{e}^{-B_T \eta^2}. \tag{4}$$

Rouse, Yih & Humphrey (1952) also obtained similarity relations for plane and round plumes and experimentally verified their functional forms. They generated plumes with gas burners, and used thermocouples and wind-vane anemometers to measure the mean buoyancy and mean vertical velocity.

Morton, Taylor & Turner (1956) extended the analysis to non-similar situations by assuming that the entrainment rate was proportional to some local characteristic velocity. By calculating the entrainment constant from the experiments, they made predictions of the heights to which plumes can rise under different ambient conditions.

Morton (1959) examined how a source of momentum and buoyancy evolves into a plume. Since both the momentum and buoyancy are added at the source, the flow near

the source is more like a buoyant jet than a plume. However, as the flow evolves, the buoyancy overwhelms the momentum added at the source and after a certain distance from the source the flow is governed by buoyancy alone. The distance over which this evolution occurs can be characterized by using the Morton lengthscale L_M given by (also see Kotsovinos & List 1977 and Baker 1980)

$$L_M = M_0^{3/4}/F_0^{1/2}, \tag{5a}$$

where M_0 and F_0 are the specific momentum and buoyancy at the source and are defined by

$$M_0 = 2\pi \int_0^{r_0} W^2 r \, dr, \quad F_0 = 2\pi \int_0^{r_0} Wg \frac{\Delta\rho}{\rho} r \, dr, \tag{5b, c}$$

where r_0 is the source radius. The present as well as other studies show that the plume-like behaviour is achieved for at least $z/L_M > 5$.

George, Alpert & Tamanini (1977) measured the mean and turbulence quantities in a plume using hot-wire anemometry with modern digital techniques. They used a two-wire probe to measure the temperature and velocity. It was found that about 15% of the total vertical heat transport was contributed by turbulence. Nakagome & Hirata (1977) also made similar measurements in an independent effort, but obtained lower values of temperature and velocity intensities than George *et al.* (1977).

Beuther (1980, see also Beuther & George 1982) used a cross-wire to measure up to fourth moments for a round plume in a stably stratified environment. He found that the stable stratification made the mean velocity and buoyancy profiles narrower. Ogino *et al.* (1980) used hot films and thermocouples to measure the centreline decay rates of velocity and temperature in round buoyant jets in both the neutral and stratified environments. Shabbir & George (1985, 1987) reported hot-wire measurements for a round plume. Papanicolaou & List (1987) used thermistor probes to measure the temperature field in buoyant jets. Papanicolaou & List (1988) carried out a more comprehensive set of measurements using LDA and laser-induced fluorescence technique. They measured both the buoyant jet and the buoyant plume regions. Papantoniou & List (1989) reported results on the large-scale structure of far-field buoyant jets.

Although existence of similarity has been confirmed in these experiments, there has been some disagreement about the centreline values of the mean velocity and buoyancy profiles as well as the plume spreading rate. Chen & Rodi (1980) (see Rodi 1986 for an updated review) reviewed the existing experimental data on plumes and recommended profiles which were very close to those of George *et al.* (1977). List (1982) in his review suggested that none of the measurements for round geometry, except his group's, have been taken in the fully developed plume region. He also pointed out that none of these studies equated the integrated buoyancy flux with the source buoyancy flux. The buoyancy flux, F, which directly appears in the similarity relations, was obtained in these studies by integrating the measured temperature and velocity profiles. This could result in some error since the probes used, hot wires, do not have the ability to resolve flow reversals believed to be present at the outer edges of the flow.

1.3. *Objectives of the present work*

From the above survey it is clear that there is a need of comprehensive data on neutral-environment round plumes which can resolve the differences in the various experiments and address the issues raised above regarding the documentation of the source conditions. This was the first objective of this study. Since for an ideal gas in a neutral

environment the conservation of energy also implies the conservation of buoyancy (see Chen & Rodi 1980), the energy and buoyancy integrals should equal the values for these quantities at the source. In the present experiment source conditions were carefully monitored to obtain the rate at which buoyancy was added at the source. The two-wire probe (consisting of a hot-wire and a cold-wire) was used to achieve this first objective since it involves smaller error for the velocity measurement than the three-wire probe (consisting of an x-wire and a cold wire). The second objective of the study was to provide more detailed measurements which can shed some light on the structure of turbulence in plumes and help identify the effect of buoyancy on turbulence. For this purpose a three-wire probe was used to measure the temperature and the two velocity components. This allowed determination of various moments up to third order which provide information about the turbulent transport of momentum and thermal energy. The budgets of the mean momentum and energy differential were determined to see how well the various terms in these equations balance. Balances of turbulent kinetic energy and temperature variance transport equations were also determined. The rates of mechanical and thermal dissipation are obtained as the closing entries in these balances. These balances show which physical phenomena dominate the different regions of the flow. The turbulent kinetic energy budget is used to study the direct influence of buoyancy on turbulence by looking at the relative magnitude of the buoyancy production term.

2. Analytics

2.1. *Governing equations*

The coordinate system for analysing the round buoyant plume is sketched in figure 1. The vertical velocity and direction are represented by W and z respectively while U and r denote the corresponding radial values. The fluctuating values are denoted by lower-case letters, e.g. fluctuating vertical velocity by w and fluctuating temperature by t. The gravitational vector is chosen to correspond with the negative z-direction.

The mean continuity, vertical momentum, and buoyancy equations, within the Boussinesq approximation and after neglecting the viscous diffusion (justified for high-Reynolds-number flow), are given by

$$\frac{1}{r}\frac{\partial rU}{\partial r}+\frac{\partial W}{\partial z}=0, \tag{6}$$

$$U\frac{\partial W}{\partial r}+W\frac{\partial W}{\partial z}=-\frac{1}{r}\frac{\partial}{\partial r}(r\overline{uw})-\frac{\partial}{\partial z}(\overline{w^2}-\overline{u^2})+g\beta\Delta T, \tag{7}$$

$$U\frac{\partial}{\partial r}(g\beta\Delta T)+W\frac{\partial}{\partial z}(g\beta\Delta T)=-\frac{1}{r}\frac{\partial}{\partial r}(rg\beta\overline{ut})-\frac{\partial}{\partial z}(g\beta\overline{wt}), \tag{8}$$

where β is the coefficient of thermal expansion and for an ideal gas is equal to the reciprocal of the gas temperature. Note that the term $(\partial/\partial z)\overline{u^2}$ in (7) represents the contribution due to the streamwise pressure gradient term $(-1/\rho)(\partial P/\partial z)$ and has been obtained by integrating the radial momentum equation (see e.g. Hussein, Capp & George 1994). In writing the buoyancy equation it was assumed that the ambient temperature is constant so that the local temperature T was replaced by the local buoyancy $g\beta(T-T_\infty)=g\beta\Delta T$.

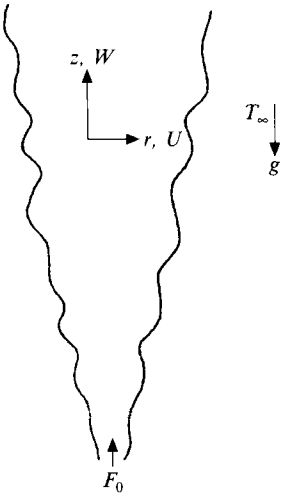

FIGURE 1. Nomenclature.

The similarity relations for the mean buoyancy and velocity are given by Batchelor (1954). For the round geometry the similarity form of the variables is given by

$$\eta = \frac{r}{z}, \quad g\beta\Delta T = T_s f_T(\eta), \quad W = W_s f_W(\eta), \quad W_s = F^{1/3} z^{-1/3}, \quad T_s = F^{2/3} z^{-5/3}. \tag{9}$$

The other moments, involving temperature and velocity, scale in a similar fashion, e.g. $g\beta\overline{wt} = W_s T_s f_{wt}(\eta)$ and $\overline{uw} = W_s^2 f_{uw}(\eta)$. (Note that we are representing the similarity functions by the symbol f with the subscript indicating the statistical quantity.)

The temperature variance and turbulence kinetic energy equations will be needed later on. Their derivation can be found in standard texts on turbulence and here there final form is given. The temperature variance equation for a round plume is

$$U\frac{\partial}{\partial r}\left(\frac{\overline{t^2}}{2}\right) + W\frac{\partial}{\partial z}\left(\frac{\overline{t^2}}{2}\right) = -\frac{1}{2}\left\{\frac{1}{r}\frac{\partial}{\partial r}(r\overline{ut^2}) + \frac{\partial}{\partial z}(\overline{wt^2})\right\} - \overline{ut}\frac{\partial T}{\partial r} - \overline{wt}\frac{\partial T}{\partial z} - \epsilon_t. \tag{10}$$

The above equation states that the advection of temperature variance is balanced by the turbulent diffusion of the temperature fluctuations, the turbulence production due to mean temperature gradients, and the molecular dissipation. The diffusion term merely redistributes energy from one point in the flow field to another. The gradient production term transfers energy from the mean flow to turbulence. And finally the dissipation term represents the rate of dissipation of energy into heat through molecular action and represents a loss of energy to turbulence.

The turbulent kinetic energy equation for a buoyant plume is

$$U\frac{\partial}{\partial r}\left(\frac{\overline{q^2}}{2}\right) + W\frac{\partial}{\partial z}\left(\frac{\overline{q^2}}{2}\right) = -\frac{1}{2}\left\{\frac{1}{r}\frac{\partial}{\partial r} r\left(\overline{uq^2} + \frac{\overline{up}}{\rho}\right) + \frac{\partial}{\partial z}\left(\overline{wq^2} + \frac{\overline{wp}}{\rho}\right)\right\}$$

$$-\overline{u^2}\left(\frac{\partial U}{\partial r} + \frac{U}{r}\right) - \overline{uw}\frac{\partial U}{\partial z} - \overline{uw}\frac{\partial W}{\partial r} - \overline{w^2}\frac{\partial W}{\partial z} + g\beta\overline{wt} - \epsilon. \tag{11}$$

This equation implies that the advection of turbulent kinetic energy is balanced by the

turbulent and pressure diffusion, the production due to the mean velocity gradients, the production due to turbulent buoyancy flux, and the viscous dissipation.

All the terms in these equations, except the dissipation rates, were measured directly. The axisymmetry assumptions of $\overline{u^2} = \overline{v^2}, \overline{wv^2} \approx \overline{wu^2}$ were used in carrying out the budget of equation (11) and were verified by rotating the x-wire by 90° in preliminary measurements taken at a few radial locations. The mechanical and thermal dissipation rates will be obtained as the closing terms in the balances of these equations.

Since, at present, there is no method of measuring the pressure diffusion terms it was decided to make an estimate of these. For this purpose the model of Lumley (1978) was used, which gives $\overline{pu_i} = -\frac{1}{5}\overline{q^2 u_i}$ (where $q^2 = u^2 + v^2 + w^2$). It is realized that there is no experimental verification of the above relation, but at the same time it is believed that it is better to use this estimate rather than just setting the pressure diffusion equal to zero. This also means that the term labelled 'dissipation', to be shown later in the kinetic energy balance, is really the sum of the dissipation rate, the errors due to the above assumption and the measurement errors present in the other terms of the kinetic energy equation.

2.2. *Integral constraints for a neutral environment*

The mean buoyancy equation (8) can be integrated across the flow to obtain

$$F = 2\pi \int_0^\infty g\beta(W\Delta T + \overline{wt})\, r\, \mathrm{d}r = \text{constant} = F_0, \tag{12}$$

where F_0 is the rate at which buoyancy is added at the source. The second term inside the integral is the turbulent contribution to the total buoyancy flux. This integral constraint implies that for an ideal gas plume, in a neutral environment, the buoyancy flux is conserved. This integral constraint must be satisfied by any experiment to within a certain experimental uncertainty. It will be shown in §4.5 that the present experiment satisfies this constraint to within 10%.

The momentum equation (7) can also be integrated across the flow to obtain

$$\frac{\mathrm{d}}{\mathrm{d}z}\left\{2\pi \int_0^\infty [W^2 + \overline{w^2} - \overline{u^2}]\, r\, \mathrm{d}r\right\} = 2\pi \int_0^\infty (g\beta\Delta T)\, r\, \mathrm{d}r, \tag{13}$$

where the contribution due to turbulence has been retained. For later use the above equation is non-dimensionalized by the source momentum flux M_0 and the lengthscale L_M, given by (5), to obtain

$$\frac{\mathrm{d}}{\mathrm{d}\xi}\left\{\frac{2\pi}{M_0} \int_0^\infty [W^2 + \overline{w^2} - \overline{u^2}]\, r\, \mathrm{d}r\right\} = 2\pi \frac{L}{M_0} \int_0^\infty (g\beta\Delta T)\, r\, \mathrm{d}r, \tag{14}$$

where $\xi = z/L_M$. The above equation shows that the momentum flux changes with vertical distance. Again it will be shown that the present experiment satisfies this constraint within experimental error.

2.3. *Stratification of the ambient surroundings*

If the ambient temperature T_∞ changes with height (i.e. $T_\infty = T_\infty(z)$), then (8), becomes

$$U\frac{\partial}{\partial r} g\beta\Delta T + W\frac{\partial}{\partial z} g\beta\Delta T = -\frac{1}{r}\frac{\partial}{\partial r}(rg\beta\overline{ut}) - \frac{\partial}{\partial z}(g\beta\overline{wt}) - W\frac{\mathrm{d}}{\mathrm{d}z}(g\beta T_\infty). \tag{15}$$

The extra term $W(\mathrm{d}/\mathrm{d}z)(g\beta T_\infty)$ arises due to the ambient stratification (see e.g. Batchelor 1954). Integrating (15) gives the following integral constraint:

$$\frac{\mathrm{d}}{\mathrm{d}z}\left[2\pi\int_0^\infty g\beta(W\Delta T+\overline{wt})\,r\,\mathrm{d}r\right]=-g\beta\frac{\mathrm{d}T_\infty}{\mathrm{d}z}2\pi\int_0^\infty Wr\,\mathrm{d}r. \tag{16}$$

We immediately see that for the neutral environment the right-hand side is zero and (16) reduces to (12). On the other hand, if $\mathrm{d}T_\infty/\mathrm{d}z$ is not zero, the entrainment of progressively lighter or heavier fluid (as measured by the integral on the right-hand side) decreases or increases the buoyancy.

In laboratory simulations of plumes some degree of stratification is always present. This is because of the finite size of the facilities and the fact that the duration of such experiments is several hours ($\approx$ 10 h). As a consequence, an inversion layer builds near the ceiling and it may or may not reach an equilibrium height above the zone of measurement.

Equation (16) provides us with a criterion to determine if a particular ambient surrounding must be regarded as stratified. Multiplying (16) by z/F_0, in order to make it dimensionless, we have

$$\frac{z}{F_0}\frac{\mathrm{d}F}{\mathrm{d}z}=-\frac{z}{F_0}g\beta\frac{\mathrm{d}T_\infty}{\mathrm{d}z}2\pi\int_0^\infty Wr\,\mathrm{d}r. \tag{17}$$

For a neutral environment $(z/F_0)(\mathrm{d}F/\mathrm{d}z)=0$. For laboratory simulation of a neutral environment we must have $(z/F_0)(\mathrm{d}F/\mathrm{d}z)\ll 1$ to ensure that the buoyancy integral is nearly independent of height as required for the neutral case. In §4.2 it will be shown that the above criterion is satisfied for the present experiment. (Note that this criterion is in addition to the requirement that $F=F_0$.)

3. Experiment

3.1. *Facility*

The plume generator is the same as that used by George *et al.* (1977) and by Beuther & George (1982). The heat source consisted of two sintered bronze discs which were heated with eight electric heaters (1500 W Watlow fire cartridges). Air from a compressed air line was first passed through these heated discs, and then through a set of screens, before finally exiting through a 12:1 contraction ratio nozzle. This resulted in an exit profile which was uniform outside the wall boundary layer to within 2%. The turbulence intensity at the exit was typically 0.5%. The space between the outer casing and the nozzle assembly was filled with silica gel for insulation purposes.

A feedback thermocouple, placed at the nozzle exit, was connected to an Electromax temperature controller. Under typical operating conditions, about two hours were required for the generator to reach thermal equilibrium. However, data collection was not started until after the plume had been running for about four hours. The variation in the exit temperature was ± 1 °C over this period compared to the nominal operating value of 292 °C.

The plume facility is schematically shown in figure 2. A square screen enclosure was placed around the plume which was 2 m × 2 m in cross-section and 5 m in height. Thus the enclosure was far enough from the flow not to interfere with it (see Appendix A).

During the course of this study it was also discovered that placing small circular screens around the source could significantly influence the buoyancy, and velocity

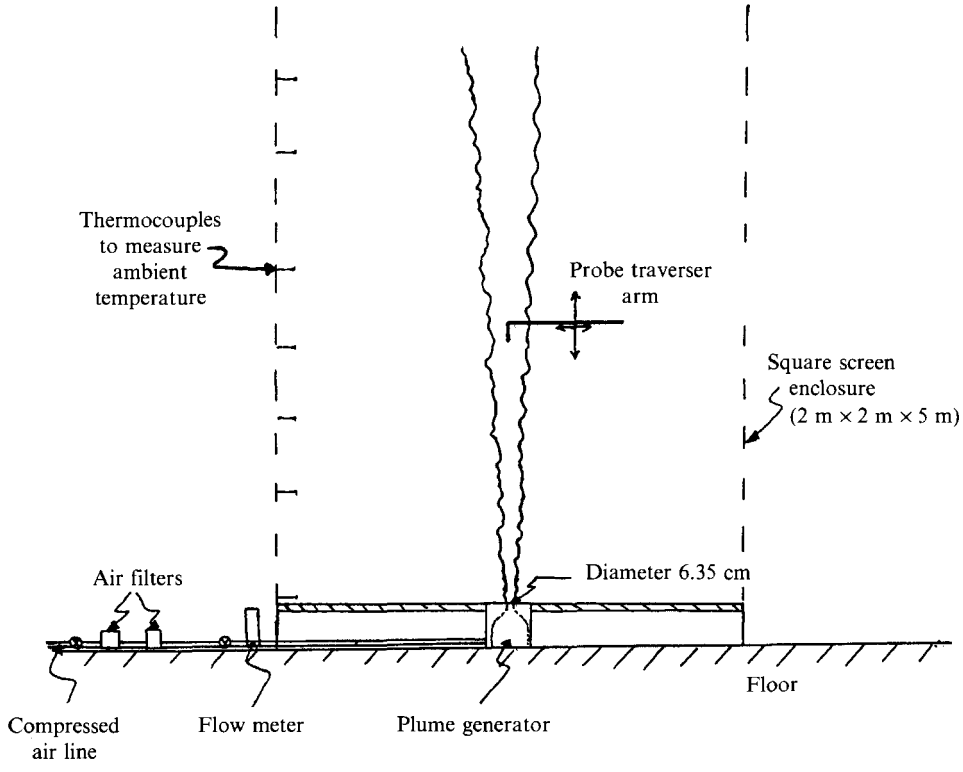

FIGURE 2. Sketch of the facility.

profiles and could act as a source of discrepancy between the various investigations. (The details of this issue are given in Appendix A.) Such screens are employed in order to prevent the flow from deflecting or moving off-centre. No such screens were used in the present study.

The dimensions of the room housing the facility were 6 m × 6 m × 10 m and it was completely shut off for the duration of the experiment. This was done in order to prevent the flow from being disturbed from cross-draughts which might arise from the heating, ventilation and air conditioning system. A flow visualization study was also carried out to confirm that there was no plume drift.

3.2. *Instrumentation*

Two kinds of hot-wire probes were used to measure the velocity and temperature fields. The first was a two-wire parallel probel (DANTEC 55P76). The leading wire was used as a cold wire to measure the temperature. It had a diameter of 1 μm and a sensitive wire length of 1.2 mm. It was operated in the constant-current mode with a heating current of 0.3 mA to ensure that its velocity response was negligible. The bottom wire was used in the constant-temperature mode to measure velocity. The sensor had an overall length of 3 mm. It was etched at the centre to give an effective length of 1.25 mm and had a diameter of 5 μm. In order to get an optimum response for both the velocity and the temperature from this wire, an overheat ratio of 0.4 was used.

The second probe used was a combination of a cross-wire and a temperature wire. The temperature wire was again 1 μm in diameter and was heated with a current of 0.15 mA. The x-wire was made of 5 μm gold-plated wire and had a length-to-diameter

ratio of 125. All the velocity sensors were operated in the constant-temperature mode using DANTEC 55M anemometer systems. For the temperature wire the 55M20 bridge was used with the 55M01 system.

To check the axisymmetry of the flow and to locate the plume centre, an array of sixteen thermocouples was used which were arranged in a 4×4 grid. The scanner used for acquiring data from these thermocouples was made using 4 mV conditioners manufactured by Analog Devices (Model 2B54A). These conditioners were specially designed for thermocouple applications. A gain of 1000 was employed so that the millivolt signal from the thermocouples was converted into volts. The scanner was driven by TTL logic and was interfaced with a PDP 11/34 mini-computer. The output from the scanner was sampled and digitized using a 16-bit A/D converter. The scanner permitted taking as many as 400 samples per second. However, the fastest rate used in the experiments was 32 samples per second. All the thermocouples used in the experiment were copper–constantan and were ice referenced. The outputs from all the anemometers and signal conditioners were digitized by a 16-bit A/D converter interfaced with the PDP 11/34.

The integral timescale of the flow was estimated to be 0.2 s. This implied that the data sampling rate need not be greater than 5 samples per second since the additional samples would not contribute to the statistical convergence. Therefore, the sampling rate was set at 4 samples per second. For each data point 2048 samples were taken and this gave a total averaging time of about 17 minutes per data point. For a stationary Gaussian signal this corresponds to a relative error of 1 % for the mean values.

3.3. *Calibration schemes*

The constant-current wire gave a linear response to the temperature changes. Since for the velocity wire the output voltage was a function of both the velocity and the temperature it was handled by expressing the wire Nusselt number, Nu, as a function of the Reynolds number. In particular

$$Re = \sum_{n=0}^{n=4} A_n Nu^{n/2}. \tag{18}$$

The coefficients A_n are temperature independent; the temperature dependence enters through the Nusselt number. For angle response of the x-wire a Hinze-type relation was used which incorporated a velocity-dependent k-factor, i.e.

$$\frac{U_{eff}}{U_0} = [\cos^2\phi + k^2(U_0)\sin^2\phi]^{1/2}, \tag{19}$$

where U_{eff} is the effective cooling velocity, U_0 is the flow velocity, and ϕ is the angle between the flow velocity and the normal to the wire. For details of these calibrations see George, Beuther & Shabbir (1989) and Shabbir, Beuther & George (1994).

The calibration of hot wires was carried out at the exit of the plume generator where it was possible to obtain the desired velocities and temperatures. It was found to be more efficient to first heat the plume generator to a particular temperature, and then vary the velocity starting from a low velocity and then gradually increasing it. Whenever velocity and temperature were changed, sufficient time was provided for the plume generator to reach thermal equilibrium. The reference temperature was obtained with a copper–constantan thermocouple placed at the source and the reference velocity was obtained by performing a mass balance on a rotameter in the inlet line which in turn had been calibrated using LDA and wet-meters.

Calibration of the wires was done both before and after the experiment. Normally the velocity calibrations were found to be very stable. However, the temperature wire was sometimes found to drift appreciably, presumably related to the stability of the DANTEC 55M20 bridge. All such data were discarded.

3.4. *Errors in measurements*

There are three primary sources of error in an x-wire signal at low velocities: rectification; cross-flow; and lack of directional sensitivity when the flow velocity makes a large inclination angle with the wire normal. The problem of rectification is obvious for a single wire in which the flow must reverse its direction for rectification to occur. Tutu & Chevray (1975) have pointed out that rectification errors are more subtle and serious for x-wires than for single wires. They also showed that the combined effects of rectification and cross-flow lead to the under-estimation of the second and higher moments.

An additional manifestation of the rectification phenomenon is the occurrence of voltage pairs which could not be resolved into velocity pairs from the angle calibration. In other words, the instantaneous voltage pairs obtained do not lie in the calibrated region and can not be inverted by equation (19). For such data, the word 'dropout' is probably a more accurate description than 'rectification'. Dropout is usually caused by a high intensity in the u- or v-component and is especially troublesome when the mean velocity is low. As noted by Beuther (1980) 'This is because wires are fairly insensitive to direction at low velocities and any small measurement error (electronic noise, prong support interference, velocity component perpendicular to the x-wire plane, wake of one wire on the other, or a velocity or temperature gradient between the wires) can create a large error in the output'. The dropout was small in the central core of the plume but was as big as 40% at its outer edges.

Since the dropped data points are associated with the low velocities, the dropout would tend to bias the velocity statistics toward the higher side. It should also be noted that, like the dropout, the flow reversals on the wire are also associated with low mean velocities. It is very difficult to quantify the combined effects of all these errors in the current experiment. As a word of caution it is recommended that all the third moments and the balances for the second moments must be regarded as qualitative in nature rather than as quantitative for values of η greater than about 0.15.

4. Results

4.1. *Source conditions*

An accurate knowledge of the source conditions is essential to check whether or not the experiment conserves buoyancy. Also the rate at which buoyancy is added at the source appears in all the similarity relations. In view of the fact that plumes in stratified environments also satisfy similarity relationships using the local buoyancy integral, it is more accurate to use the source buoyancy (which must be conserved for the neutral environment) than the buoyancy obtained by integrating the measured velocity and temperature profiles.

Schlieren visualization showed that the flow was not laminar after about one diameter. Source conditions for the two-wire probe, three-wire probe, and thermocouple experiments are given in table 1. Current and other experiments show that the buoyant jet reaches an asymptotic plume-like condition for $\xi(= z/L_M) > 5$. For the source conditions of this study, this criterion is met as ξ ranges from 6.5 to 16. The centreline values of buoyancy, non-dimensionalized by $zM_0^{1/2}/F_0$, can be plotted as a

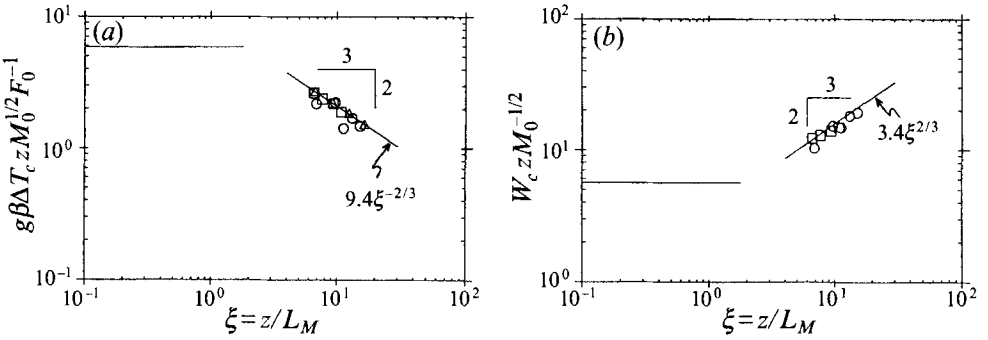

FIGURE 3. (*a*) Normalized mean buoyancy and (*b*) normalized mean vertical velocity, along the centreline of the buoyant plume plotted as a function of the normalized vertical distance z/L_M: △, thermocouple data; □, two-wire probe data; ○, three-wire probe data.

Experiment	Diameter D (m)	T_0 (°C)	U_0 (m s^{-1})	F_0 (m^4 s^{-3})	M_0 (m^4 s^{-2})
Two-wire probe	0.0635	295	0.98	0.0127	0.0030
Three-wire probe and thermocouple	0.0635	295	0.86	0.0115	0.0023

TABLE 1. Flow parameters at the plume source

function of non-dimensional vertical distance ξ. For a buoyant jet these should follow a horizontal line and for a buoyant plume these should follow a $-\frac{2}{3}$ slope (see Morton 1959; Kotsovinos & List 1977; Baker *et al.* 1980). Figure 3(*a*) shows such a plot for the present experiments and clearly these correspond to a plume-like flow. Figure 3(*b*) shows a similar graph for the centreline vertical velocity, non-dimensionalized by $z/M_0^{1/2}$, plotted as a function of ξ. Note that for some of the locations centreline buoyancy and velocity were not measured and for such cases the next point off the centreline axis was used. Because of this there is some scatter in the data points shown in these figures. The curve fits to the data of figure 3 are given by

$$\frac{g\beta\Delta T_c z M_0^{1/2}}{F_0} = 9.4\xi^{-2/3}, \quad \frac{W_c z}{M_0^{1/2}} = 3.4\xi^{2/3}.$$

4.2. *Ambient conditions*

Beuther & George (1982) and Beuther (1980) have shown that a small stratification of the ambient fluid can cause a significant loss or gain of buoyancy depending on the sign of the right-hand side of (16) and hence can appreciably change the shape of the profiles. In the experiment of Beuther (1980) the ambient fluid was stably stratified and the data collapsed when plotted using the similarity variables provided that the local value of the buoyancy flux was used. His measurements showed that the stable stratification made the mean profiles narrower and higher.

None of the studies reported in the literature have monitored or documented the ambient temperature changes with the exception of Ogino *et al.* (1980) and Kotsovinos (1985). In the present experiment the ambient temperature was continuously monitored by using seven copper–constantan thermocouples placed at different heights. Figure 4 shows the change in ambient temperature as a function of both height and time for one of the experimental runs. It is seen that for the first two hours of operation a significant

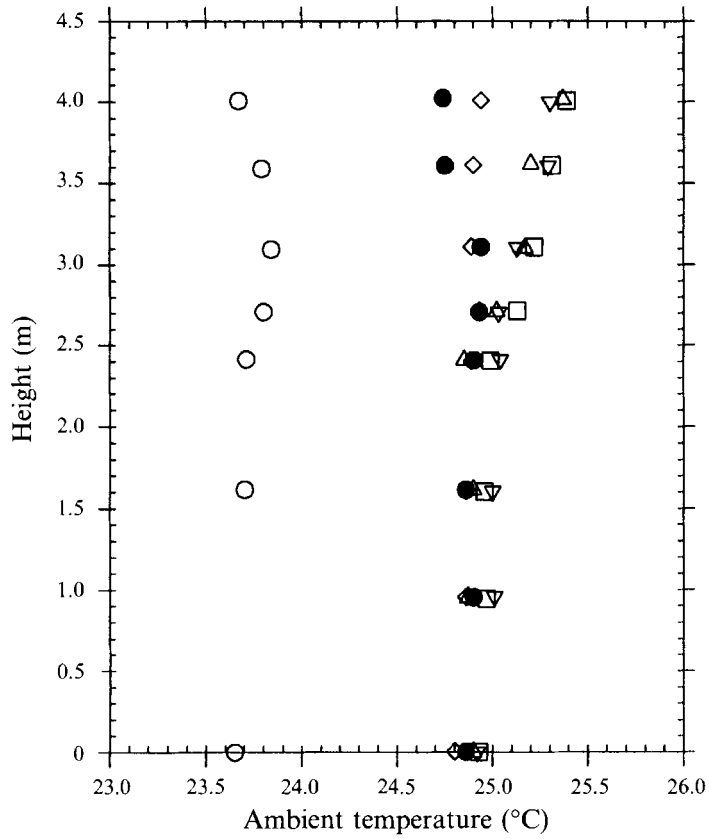

FIGURE 4. Change in ambient surrounding temperature shown as a function of vertical distance and time for one of the experimental runs: ○, 0:00 hours; △, 3:20 hours; □, 3:30 hours; ▽, 4:30 hours; ◇, 6:30 hours; ●, 8:30 hours.

change in the temperature occurs. However, after this it changes very little, especially over the heights where the measurements were taken.

According to the criterion established in §2.3 for avoiding stratification effects,

$$-\frac{z}{F_0} g\beta \frac{\mathrm{d}T_\infty}{\mathrm{d}z} 2\pi \int_0^\infty Wr\,\mathrm{d}r \ll 1. \tag{20}$$

For this experiment the value of the above relation is 0.003 which is much smaller than 1. For the experiment of Beuther (1980) the value of (20) was about 0.36. Based on these we can confidently say that the measurements reported herein are taken in a neutral environment.

4.3. *Mean flow results*†

The mean buoyancy profile is shown in figure 5(*a*). The closed symbols refer to the two-wire probe measurements and the open symbols refer to the three-wire probe measurements. The curve shown is the Gaussian fit to the data and is given by

$$g\beta\Delta T F_0^{-2/3} z^{5/3} = f_T(\eta) = 9.4\exp(-68\eta^2). \tag{21}$$

† Tables of data taken at various r/z and z values with the two-wire and three-wire probes for $g\beta\Delta T F_0^{-2/3} z^{5/3}$, $WF_0^{-1/3} z^{1/3}$, $g^2\beta^2\overline{t^2}F_0^{-4/3} z^{10/3}$, $g\beta\overline{wt}F_0^{-1} z^2$, $\overline{w^2}F_0^{-2/3} z^{2/3}$, together with data for $g\beta\overline{ut}F_0^{-1} z^2$, $\overline{u^2}F_0^{-2/3} z^{2/3}$ and $\overline{uw}F_0^{-2/3} z^{2/3}$ for the three-wire probe only, are obtainable from the authors or the JFM Editorial Office.

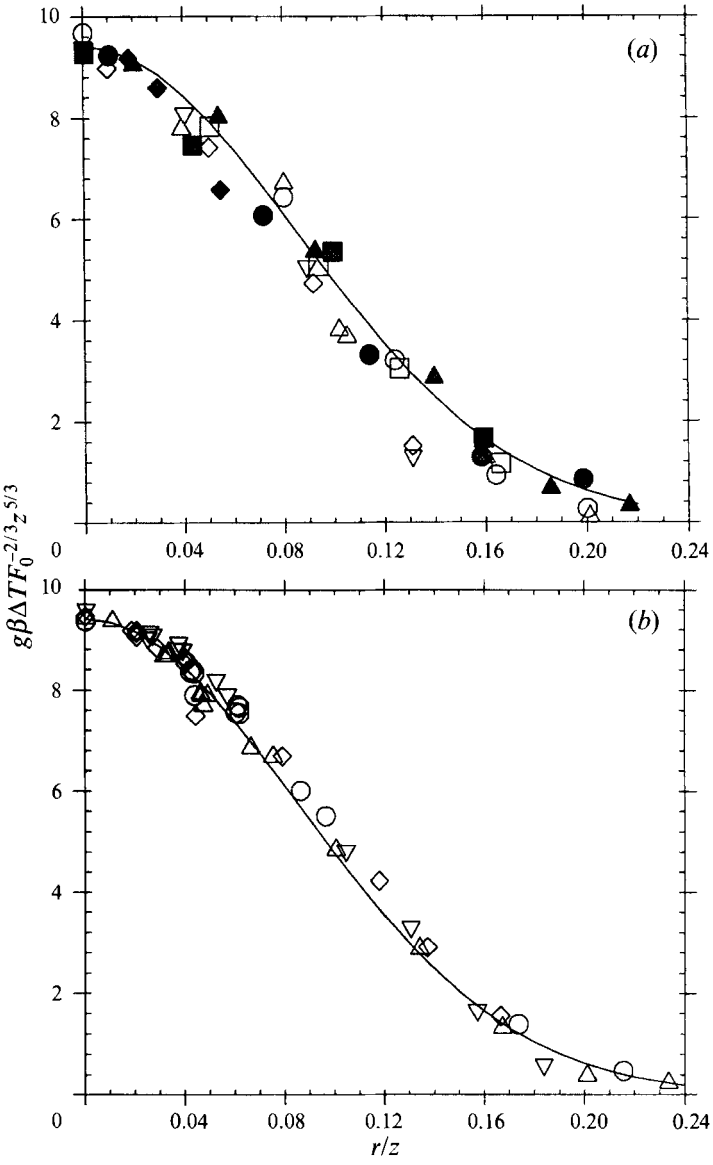

FIGURE 5. (*a*) Profile of mean buoyancy in similarity variables. Solid symbols refer to the two-wire probe measurements and open symbols refer to the three-wire probe measurements. ■, $z/D = 11.81$; ●, $z/D = 13.7$; ▲, $z/D = 16.77$; ◆, $z/D = 19.5$; □, $z/D = 10.55$; ○, $z/D = 14$; △, $z/D = 17.3$; ▽, $z/D = 20.31$; ◇, $z/D = 23.46$. (*b*) Profile of mean buoyancy in similarity variables, as measured with thermocouples. ◇, $z/D = 10$; ○, $z/D = 14$; △, $z/D = 19$; ▽, $z/D = 25$.

(Note that preference was given to the two-wire probe measurements while performing the curve fit.) The data collapse is very reasonable and gives confidence that the plume is fully developed at the locations where the measurements are taken. The centreline value of 9.4 is slightly higher than the value of 9.1 recommended by George *et al.* (1977) who used the same instrumentation but calculated the buoyancy flux by integrating the measured velocity and temperature profiles. If, like theirs, the present data is normalized by the local buoyancy flux, then the centreline value of the mean buoyancy will be 9.0, thus indicating that the differences are attributable to errors in their

Reference	A_T	A_W	B_T	B_W	$l_{\Delta T/2}$	$l_{W/2}$	$(\overline{t^2})^{1/2}/\Delta T_c$	$(\overline{w^2})^{1/2}/W_c$
Rouse *et al.*	11.0	4.7	71	96	0.095	0.084	—	—
George *et al.*	9.1	3.4	65	55	0.104	0.112	0.38	0.28
Nakagoma & Hirata	11.5	3.89	48.1	63	0.105	0.12	0.36	0.25
Papanicolaou & List	14.28	3.85	80	90	0.093	0.0877	0.42	0.25
Chen & Rodi	9.35	3.5	65	55	0.10	0.112	—	—
Present study	9.4	3.4	68	58	0.10	0.107	0.40	0.33

TABLE 2. Summary of mean flow parameters and turbulence intensities

calculation of buoyancy. The centreline value reported here is considerably lower than the $A_T = 11.0$ reported by Rouse *et al.* (1952). Most of this difference can be attributed to the fact that they did not include the turbulence contribution to the total heat flux which can amount to as much as 18% (to be discussed later in §4.5). If this is taken into account, then their value of A_T would drop from 11.0 to 9.9, which is only 5.3% larger than what is reported here. Ogino *et al.* (1980) measured $A_T = 9.4$, which is the same value as reported here, whereas Kotsovinos (1985) reported a value of 8.8. On the other hand, Papanicolaou & List (1987, 1988) reported values of 11.11 and 14.28 respectively, the former measured with thermistor probes and the latter using the LIF technique. The value recommended by Chen & Rodi (1980) and Rodi (1986) is 9.35, which is in excellent agreement with the present experiment.

The non-dimensional half-width of the buoyancy profile, $l_{\Delta T/2}$ (defined as the location where the normalized buoyancy is half its centreline value), is 0.1. As can be seen from table 2 this is in excellent agreement with the recommendations of George *et al.* (1977), Chen & Rodi (1980), and Rodi (1986). It is approximately the same as suggested by the measurements of Rouse *et al.* (1952) and Kotsovinos (1985) but is about 8% larger than the value reported by Papanicolaou & List (1987, 1988).

The buoyancy profile measured using thermocouples is shown in figure 5(*b*). It has the same centreline value and half-width as was measured with the hot wire. This not only complements the hot-wire measurements, but also shows that the slight differences between the present study and that of Rouse *et al.* (1952) are not instrumentation related. However, there are still substantial differences between the results of this study and Papanicolaou & List (1987, 1988); their profiles are higher and narrower than those measured in the present experiment.

It should be pointed out that the measurements of Papanicolaou & List (1988) extend over larger non-dimensional axial distances (i.e. z/L_M) than in the present experiment. Therefore, it could be argued that this could be a reason for the differences between the two studies, i.e. that an overall fit for the decay of mean centreline buoyancy obtained from the Papanicolaou & List (1988) experiment would be more accurate than that obtained from the present experiment (figure 3*a*). This argument would be a valid one if the two studies measured similar decay rates in the overlapping regions of z/L_M. However, the two experiments differ within this overlapping region. The mean centreline buoyancy values of present study would have to be changed by 50% over their current values in order for them to agree with the Papanicolaou & List (1988) results. Clearly this large difference cannot be explained by the above argument.

The mean velocity profile is shown in figure 6, where the curve is the Gaussian fit to the data given by

$$WF_0^{-1/3}z^{1/3} = f_W(\eta) = 3.4\exp(-58\eta^2). \tag{22}$$

(Again note that preference was given to the two-wire probe measurements while

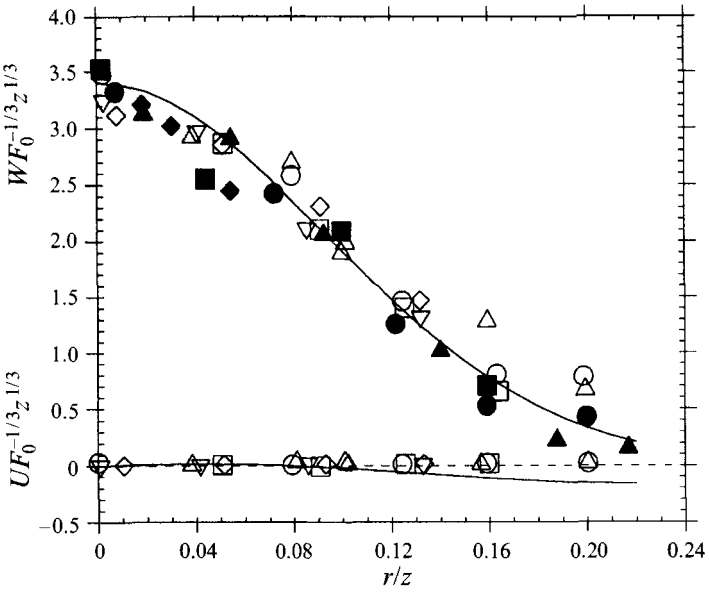

FIGURE 6. Mean vertical and radial velocity profiles in similarity variables. For meaning of symbols see caption of figure 5(*a*).

performing the curve fit.) The centreline value of 3.4 is exactly the same as reported by George *et al.* (1977) and Ogino *et al.* (1980). Note that the velocity is less sensitive to the method of evaluating the buoyancy integral than is the temperature since it varies as $F^{-1/3}$ versus $F^{-2/3}$. The value recommended by Chen & Rodi (1980) and Rodi (1986) is 3.5. As can be seen from table 2 the values reported by Rouse *et al.* (1952), Nakagome & Hirata (1977), and Papanicolaou & List (1988) are somewhat higher. We note that the differences in the mean velocity measurements between the present study and that of Papanicolaou & List (1988) are much smaller than the differences in the mean buoyancy measurements.

The non-dimensional half-width for the velocity, $l_{W/2}$ (defined as the distance from the centreline where the normalized velocity is half its centreline value), is slightly greater than 0.1 and is in excellent agreement with the findings of George *et al.* (1977), Chen & Rodi (1980), and Rodi (1986). We note that the velocity profile is wider than the buoyancy profile. This is also in agreement with the findings of Nakagome & Hirata (1977) and George *et al.* (1977) and the recommendations of Chen & Rodi (1980). The measurements of Rouse *et al.* (1952) and Papanicolaou & List (1988) show just the opposite result.

The measured radial velocity profile is also shown in figure 6. This can also be obtained from the continuity equation as

$$U = \frac{1}{r}\int_0^r \frac{\partial W}{\partial z} r\,\mathrm{d}r. \tag{23}$$

If the above equation is cast into similarity variables and if the Gaussian expression is used for the vertical velocity (i.e. (22)) we obtain the following expression for the mean radial velocity:

$$f_U(\eta) = \frac{-5}{3}\frac{1}{2B_W}\left[\frac{f_W(0)-f_W(\eta)}{\eta}\right] + \eta f_W(\eta). \tag{24}$$

From figure 6 we note that the mean radial velocity is very small compared to the mean

vertical velocity, as is assumed when making the thin-shear-layer approximation for such a flow. Also note that the continuity-inferred radial velocity becomes negative (directed inwards) after about $\eta \approx 0.10$ whereas the measured value does not. The difference can be attributed to the hot-wire cross-flow errors which are of the same order as the velocity U itself.

4.4. *Turbulence properties*

Various second moments involving temperature and velocity are shown in figure 7. All these moments are plotted in terms of the similarity variables because that is the way they appear in the equations of motion. When comparing the statistics of different flows with each other (e.g. jets versus plumes) it is sometimes more helpful to use turbulence intensities and for this reason the centreline and the peak values of these will also be mentioned. The similarity profile of temperature variance, $g^2\beta^2\overline{t^2}F_0^{-4/3}z^{10/3}$ (figure 7*a*), has a centreline value of 12.5 and has a slight off-axis peak which corresponds to a temperature intensity, $(\overline{t^2})^{1/2}/\Delta T_c$, of about 40% (subscript c stands for centreline). This value is in good agreement with the values of 43% and 44% reported by Nakagome & Hirata (1977) and Kotsovinos (1985) respectively. The measurements of Papanicolaou & List (1988) show a peak value of 42%. However, owing to substantial differences in the mean buoyancy profile between this reference and the present study, this intensity is a misleading parameter for comparison. If their concentration profile is translated into similarity variables it gives a centreline value of about 32.0 which is about three times higher than the value measured here; a very large difference. So there are substantial differences between the present study and that of Papanicolaou & List (1988) for both the mean and the turbulent buoyancy measurements.

The centreline value of the normalized vertical turbulent heat flux, $g\beta\overline{wt}F_0^{-1}z^2$, is 1.85. Measurements of George *et al.* (1977) correspond to a value of 1.90 whereas those of Papanicolaou & List (1988) correspond to a peak value of 3.0. It can be seen from figure 7(*b*) that for $\eta > 0.16$ the x-wire measurements are a factor of almost two higher than the single-wire measurements. This error is due to the dropout and poor directional response associated with x-wires at higher turbulence intensities as was discussed in §3.4. This kind of error can be seen in some of the other second moments as well. Obviously, wherever available, single-wire results are to be preferred. The correlation coefficient $\overline{wt}/(\overline{w^2}\overline{t^2})^{1/2}$ has a peak value of 0.7 at $\eta = 0.12$. It confirms the value of 0.67 measured by George *et al.* (1977). Nakagome & Hirata (1977) reported a value of 0.46 for this correlation. The measurements of Papanicolaou & List (1987, 1988) give a peak value of about 0.51. The radial turbulent heat flux $g\beta\overline{ut}F_0^{-1}z^2$, shown in figure 7(*c*), has a peak value of 0.90 at $\eta = 0.07$ and its shape is very close to the derivative of the mean buoyancy.

The normalized centreline value of vertical velocity fluctuations $\overline{w^2}F_0^{-2/3}z^{2/3}$ (figure 7*d*) is 1.1. This corresponds to a turbulent intensity, $(\overline{w^2})^{1/2}/W_c$, of about 32% which is slightly higher than the value of 28% measured by George *et al.* (1977). The value reported by Papanicolaou & List (1988) is 25%. They reported a centreline value of the mean vertical velocity of 3.85 as compared to 3.4 measured in the present investigation and this might explain the differences. If their results are translated to the similarity variables one obtains 0.90 for the centreline value for $\overline{w^2}F_0^{-2/3}z^{2/3}$, which is close to what is measured here. The centreline value of the radial velocity fluctuations $\overline{u^2}F_0^{-2/3}z^{2/3}$ (figure 7*e*) is 0.65 and corresponds to a turbulence intensity, $(\overline{u^2})^{1/2}/W_c$, of 19%. The value reported by Papanicolaou & List (1988) is about 15%. The shear stress profile, $\overline{uw}F_0^{-2/3}z^{2/3}$, is plotted in figure 7(*f*) and has a maximum value of 0.32 at $\eta = 0.07$ and

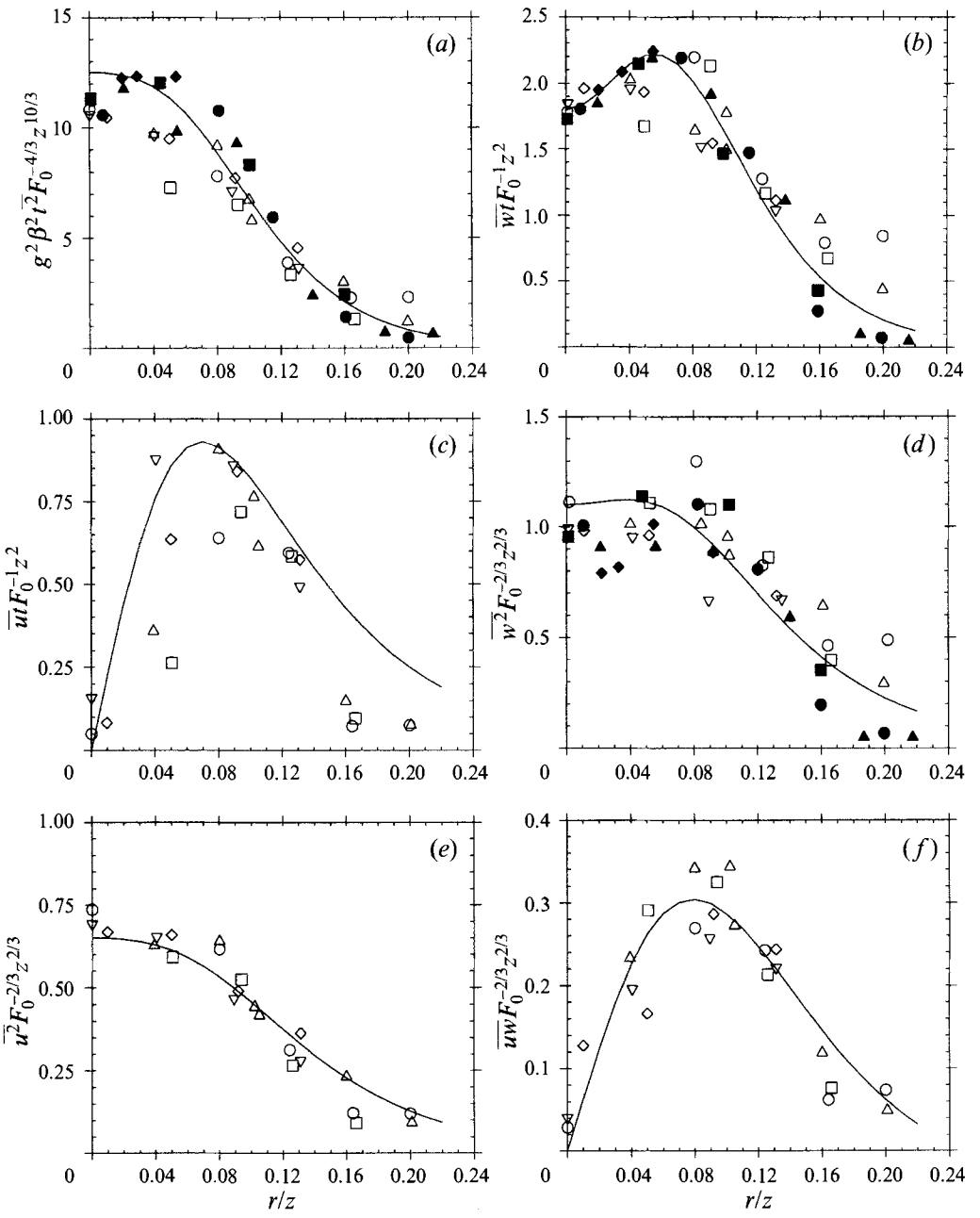

FIGURE 7. Various second-moment profiles plotted in terms of similarity variables: (*a*) temperature fluctuations; (*b*) the vertical turbulent heat flux; (*c*) the radial turbulent heat flux; (*d*) the vertical velocity fluctuations; (*e*) the radial velocity fluctuations; (*f*) the turbulent shear stress. For meaning of symbols see caption of figure 5(*a*).

its shape strongly resembles the mean velocity gradient. If normalized by the centreline value of mean vertical velocity (i.e. $\overline{uw}/W_c$) the peak value of shear stress is about 0.09. It should be noted that both shear stress and radial heat flux reported here have small finite values at the centre rather than being zero. This is due to the finite values of the various hot-wire errors for these quantities.

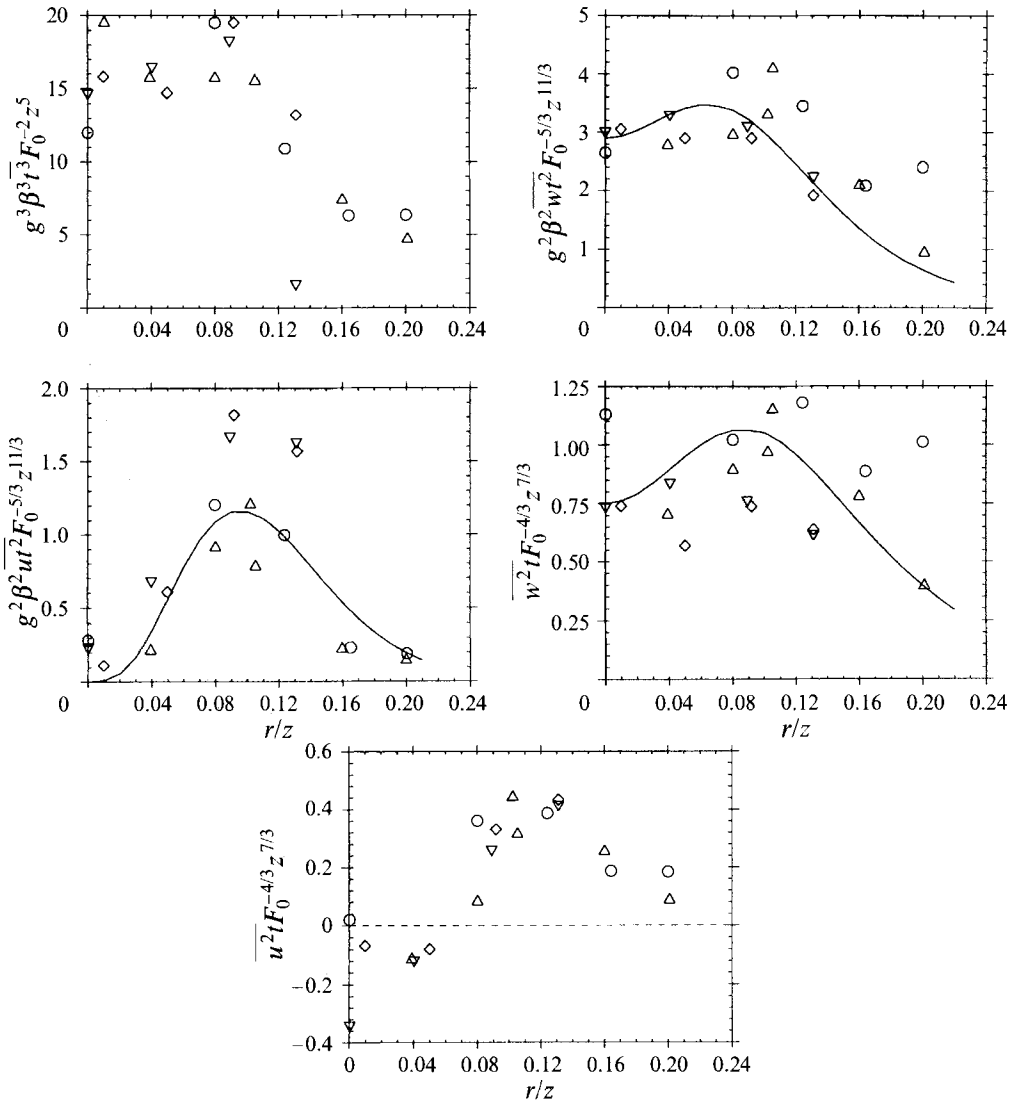

FIGURE 8. Profiles of third moments involving temperature plotted in similarity variables. For meaning of symbols see caption of figure 5(*a*).

The foregoing results can be used to calculate the turbulent Reynolds number (see Townsend 1956) $Re_T = W_c l_{W/2}/\nu_T$, where $l_{W/2}$ is the velocity half-width, and ν_T is turbulent eddy viscosity defined by

$$\nu_T = -\frac{\overline{uw}}{\partial W/\partial r}.$$

Current measurements show that Re_T has an average value of 22.5. For round wakes and jets these values are 14.1 and 32 respectively (Townsend 1956). Lumley (1971) had calculated Re_T for a plume to be 14 from the measurements of Rouse *et al.* (1952) which is very close to the wake value. The reason given by Lumley (1971) for this plume value being closer to that for a wake than for a jet was that in plumes the buoyancy causes lateral squeezing of the eddies which makes them structurally closer to those of

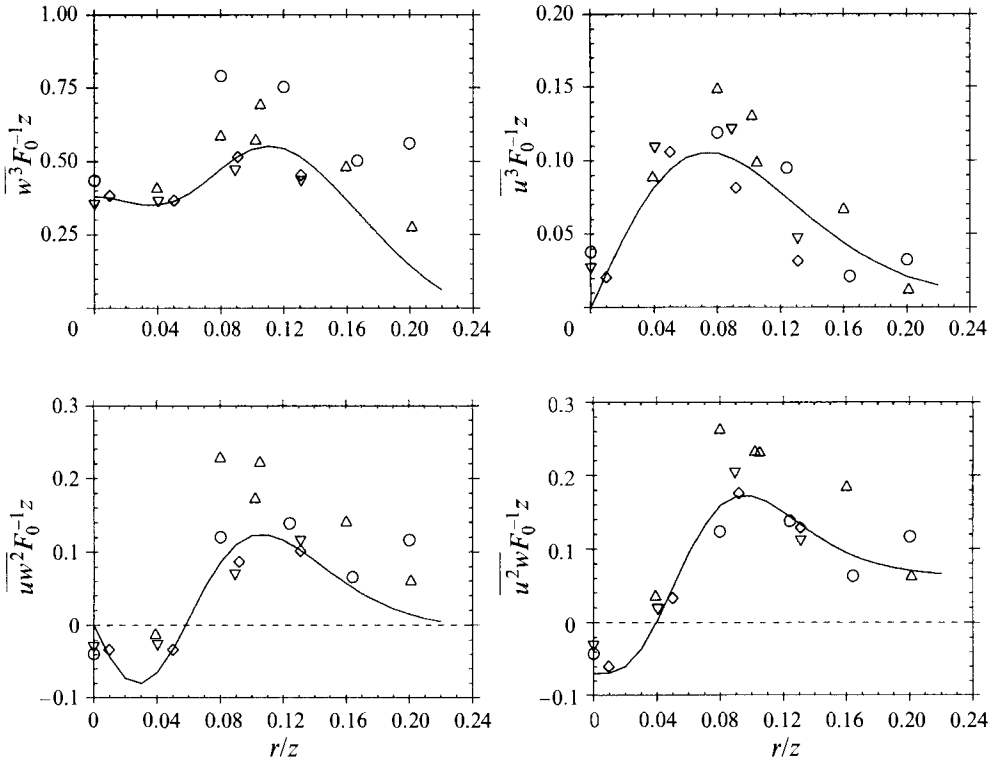

FIGURE 9. Profiles of third moments involving velocity only plotted in similarity variables. For meaning of symbols see caption of figure 5(*a*).

a wake. The current experiment shows that for a plume this value is in between the values for a wake and a jet and, therefore, a plume cannot be considered structurally closer to a wake. However, the observation of Lumley (1971) regarding the lateral squeezing of eddies in plumes still holds because the plume value is smaller than the jet value. The turbulent thermal diffusivity can also be calculated by using

$$\gamma_T = -\frac{\overline{ut}}{\partial T/\partial r},$$

and the result can be expressed in the form of a turbulent Prandtl number ν_T/γ_T. In the present experiment this value ranges from 0.7 to 1.0.

The third-order moments for the last four measurement stations are shown in figures 8 and 9. Some of these third moments will be used in balancing the temperature variance and turbulent kinetic energy equations. The moments $\overline{wt^2}$, $\overline{w^2t}$ and $\overline{t^3}$ all start from finite values at the centre and then show a slight off-axis peak before rolling off to small values. The moments $\overline{w^2u}$, $\overline{wu^2}$ and $\overline{ut^2}$ show negative values near the centreline axis. Some of the third moments show small values at the centreline rather than being zero owing to the cross-flow errors associated with the hot wires. The curves shown in these figures are the polynomial fits to the data and these are shown in Appendix B along with the fits to the higher moments. It should be noted that, where possible, preference was given to the two-wire probe measurements in doing the curve fits.

One disappointing feature of these third moments is their wide scatter. For the number of samples taken, the relative error in these is estimated to be about 10% near

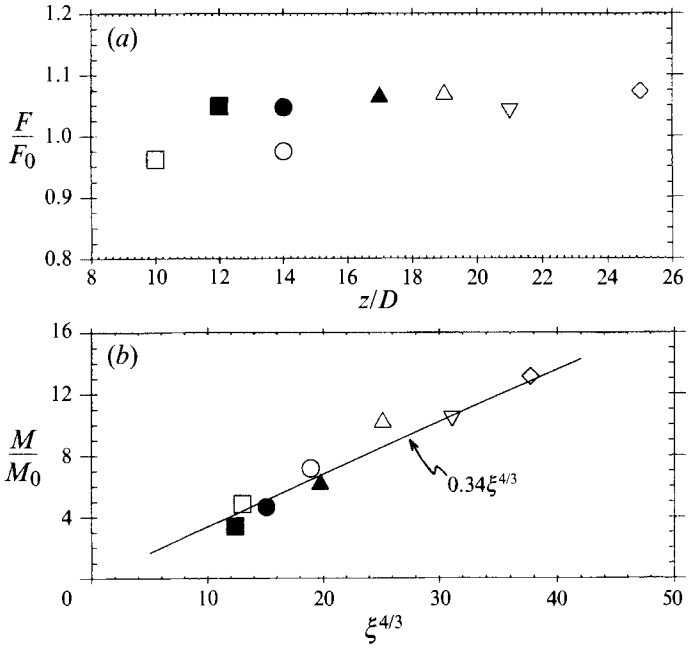

FIGURE 10. (*a*) Ratio of the total local buoyancy flux (obtained by integrating the measurements) to the source buoyancy flux plotted as a function of the vertical distance z/D. (*b*) Ratio of the mean local momentum flux (obtained by integrating the measurements) to the source momentum flux plotted as a function of the normalized vertical distance $\xi^{4/3}$. For meaning of symbols see caption of figure 5(*a*).

the centreline. This value increases away from the core as the turbulence intensity increases. It should also be noted that such scatter is also present in the other plume experiments which have been cited earlier in this paper.

4.5. *Evaluation of the integral constraints*

As was discussed in §2.2 the integral constraint arising from the mean buoyancy equation implies that the buoyancy flux should be conserved for a plume in a neutral environment. Therefore, the local values of buoyancy flux, F, at different heights were obtained by using (12). Note that this integration includes the turbulent contribution as well. Figure 10(*a*) shows the ratio of this local buoyancy to the source buoyancy, F/F_0, at various heights. It is clear that the experiment conserves buoyancy within 10%, which is within the experimental error. The turbulent contribution was found to be in the range of 15% to 18% of the total buoyancy flux. This is a substantial percentage that cannot be ignored in any integral-type analysis of this flow. This was noted by George *et al.* (1977) who had also found this contribution to be about 15%, and subsequent studies by Beuther (1980), Shabbir & George (1985) and Papanicolaou & List (1988) have confirmed this. It should be noted that the accuracy of the integration is better than might have been expected from a consideration of the hot-wire errors at large radius. This is because the temperature and velocity profiles fall rather sharply with radius so that the integrand of equation (12) is dominated by the profiles in the core region.

In order to check the integral momentum constraint, given by (14), the mean momentum flux, normalized by its source value, is plotted against $\xi^{4/3}$ in figure 10(*b*). Its derivative at a given location should equal the buoyancy acceleration at that location. The curve fit to the data gives $M/M_0 = 0.34\xi^{4/3}$. This can be differentiated to

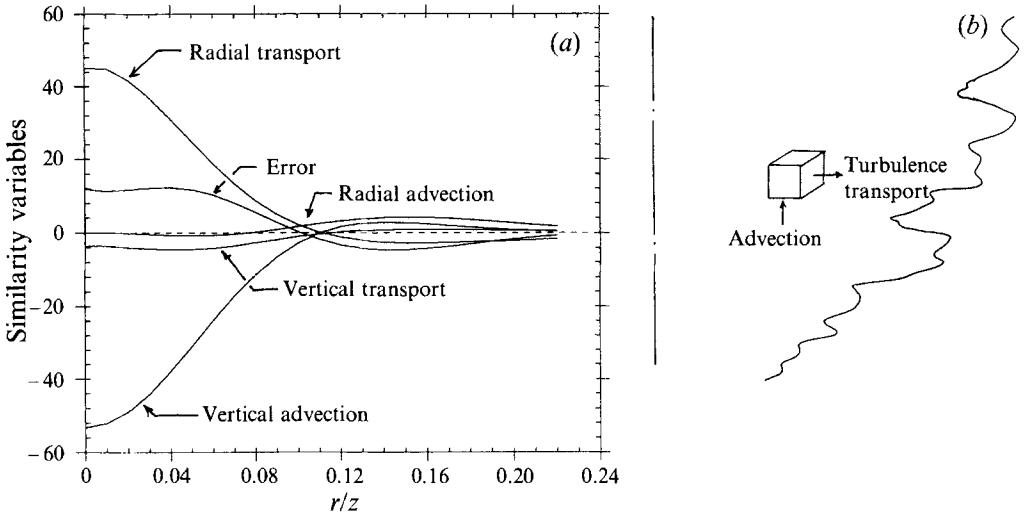

FIGURE 11. (*a*) Balance of the mean buoyancy differential equation. (*b*) Sketch showing the different zones of the plume based on the mean buoyancy differential equation balance.

Experiment	$\xi = z/L_M$	$\frac{2\pi}{M_0} \times \int_0^\infty (W^2+\overline{w^2}-\overline{u^2})\, r\, dr$	$\frac{d}{d\xi}\left\{\frac{2\pi}{M_0} \times \int_0^\infty (W^2+\overline{w^2}-\overline{u^2})\, r\, dr\right\}$	$2\pi\frac{L_M}{M_0} \times \int_0^\infty (g\beta\Delta T)\, r\, dr$
Two-wire probe	6.59	3.42	0.85	0.85
	7.65	4.67	0.98	0.89
	9.36	6.13	1.03	0.96
Three-wire probe	6.84	4.86	0.92	0.86
	9.09	7.17	0.92	0.95
	11.23	10.14	1.03	1.02
	13.17	10.53	1.03	1.07
	15.21	13.13	1.08	1.13

TABLE 3. Check of integral momentum constraint

obtain the left-hand side of (14). The results are given in table 3 and the agreement between the two sides of the momentum integral (equation (14)) is satisfactory.

The contribution $2\pi\int_0^\infty(\overline{w^2}-\overline{u^2})\,r\,dr$ to the momentum flux (see (13)) is found to be 4.6% of the mean momentum flux. This is quite small and, therefore, can be ignored in an integral type of analysis. Notice that both $\overline{w^2}$ and $\overline{u^2}$ are of the same order and if one is kept the other must also be retained.

4.6. *Balances of the mean buoyancy and momentum equations*†

The balance of the mean buoyancy equation (equation (8)) is shown in figure 11 (*a*). We observe that the radial advection term is extremely small compared to the vertical advection term. This is because the mean radial velocity is negligible compared to the

† Tables of measured data for the terms in the mean buoyancy and momentum equations for various values of η are available from the authors of the JFM Editorial Office.

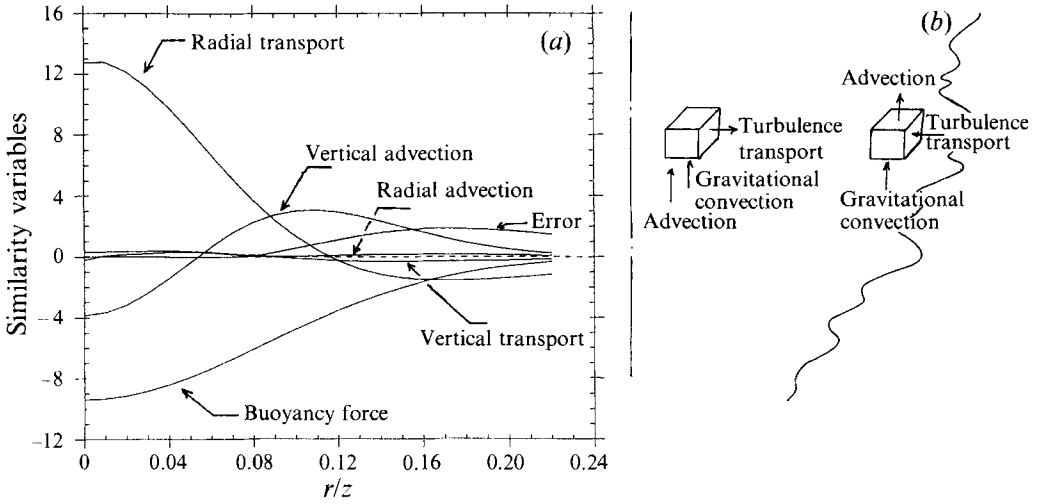

FIGURE 12. (*a*) Balance of the mean momentum differential equation. (*b*) Sketch showing the different zones of the plume based on the mean momentum differential equation balance.

vertical velocity. We also note that the vertical turbulent transport is extremely small compared to the radial turbulent transport. Note that when this equation is integrated across the flow the radial advection and radial turbulent transport terms fall out. The term labelled 'error' represents the amount which is missing from the right-hand side of (8). This error is due to the underestimation of the radial turbulent heat flux. We also observe that the relative magnitude of each term remains the same across the plume and that all the terms fall off to very small values after $\eta \approx 0.1$. In summary we can say that in a plume the mean flow advects the buoyancy in the vertical direction and turbulence transports it in the radial direction (figure 11*b*) i.e.

$$W\frac{\partial}{\partial z}(g\beta\Delta T) \approx -\frac{1}{r}\frac{\partial}{\partial r}(rg\beta\overline{ut}).$$

The balance for the mean momentum differential equation (equation (7)) is shown in figure 12(*a*). We note that, like the mean buoyancy equation, the advection in the radial direction is very small compared to the advection in the vertical direction and that the turbulent transport of momentum in the vertical direction is negligible compared to the turbulent transport in the radial direction. We also note that at $\eta = 0.06$ the vertical advection changes its sign and after $\eta \approx 0.11$ advection and turbulent transport have exchanged sides in the balance, as is depicted in figure 12(*b*). The body force, due to gravitational convection, is the second largest term in this budget. It is this term which is responsible for setting the fluid into motion and which links the mechanical and thermal flow fields. This term leads to larger velocity gradients in plumes than in jets. Increased mixing leads to increased transfer of momentum which results in wider velocity profiles in plumes than in jets. We further note that the terms in the momentum budget do not fall off to small values after $\eta \approx 0.1$ as they did for the mean buoyancy balance. We conclude that to first order the vertical advection of momentum is balanced by the turbulent transport in the radial direction and the gravitational advection, i.e.

$$W\frac{\partial W}{\partial z} \approx -\frac{1}{r}\frac{\partial}{\partial r}(r\overline{uw}) + g\beta\Delta T.$$

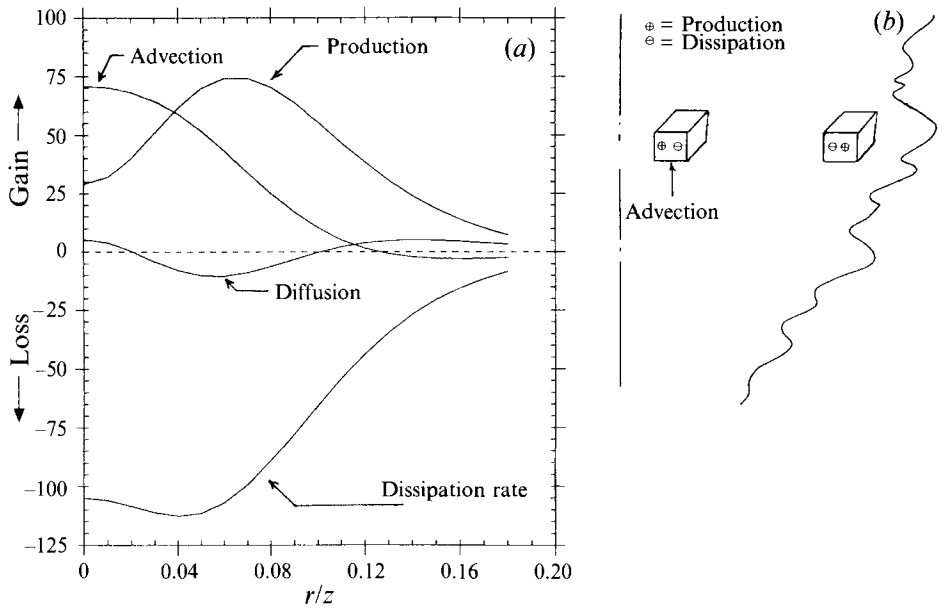

FIGURE 13. (*a*) Balance of the temperature variance, $\frac{1}{2}\overline{t^2}$, equation. (*b*) Sketch showing the different zones of the plume based on the temperature variance balance.

It should be noted that these balances are not trivial and that they further help to establish the consistency and accuracy of the experiment.

4.7. *Balances for the* $\frac{1}{2}\overline{t^2}$ *and* $\frac{1}{2}\overline{q^2}$ *equations*†

The balance of $\frac{1}{2}\overline{t^2}$ (equation (10)) is shown in figure 13(*a*). We note that the advection term forms a major portion of the budget in the central half of the flow before acquiring a small value after $\eta \approx 0.10$. Incidentally, this location approximately corresponds to the temperature half-width. At the centreline production of temperature variance is about half the magnitude of the advection but it monotonically increases until it peaks at $\eta \approx 0.07$. We note that the peak values of the advection and the production terms are about the same. The diffusion term is quite small compared to the other terms. The thermal dissipation rate ϵ_t was not measured and, therefore, is obtained as the closing term and is the largest of all the terms in the budget. Obviously a successful computation of the temperature variance by any turbulence model is crucially dependent on how accurately this dissipation rate is calculated.

The budget suggests dividing the flow into two regions. In the inner region ($\eta < 0.1$, which approximately corresponds to the temperature half-width) advection and production mechanisms provide most of the energy to temperature variance and are balanced by the dissipation rate. Obviously the flow is not in local equilibrium (i.e. production ≠ dissipation) in this region. In the outer region ($\eta > 0.1$) the production of temperature variance is balanced by the dissipation rate and the flow in this region, therefore, can be approximated to be in local equilibrium. These regions are schematically depicted in figure 13(*b*).

Figure 14(*a*) shows the turbulent kinetic energy balance and we note that the

† Tables of measured data for the terms in the temperature variance and turbulence kinetic energy equations for various values of η are available from the authors or the JFM Editorial Office.

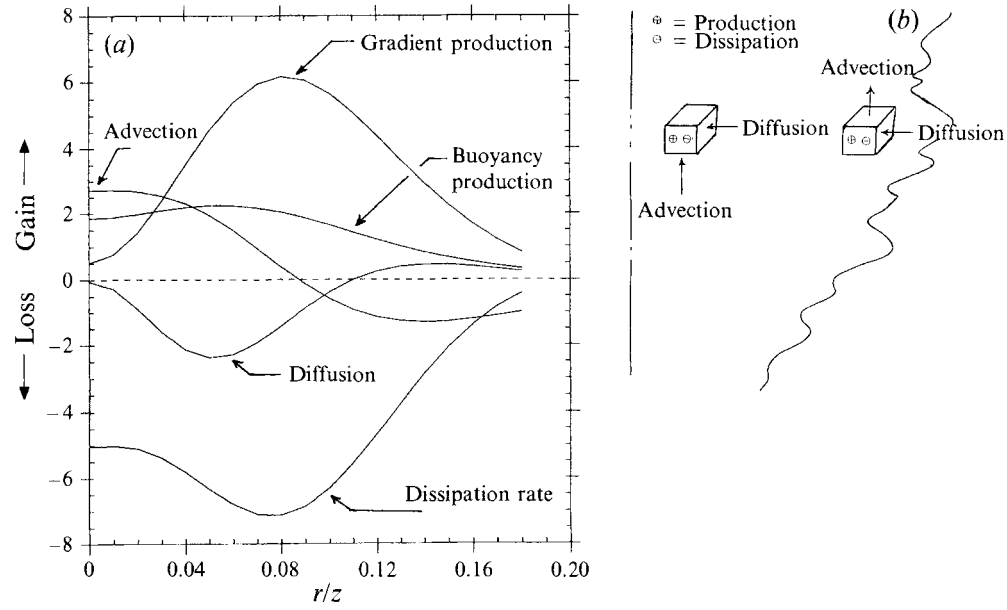

FIGURE 14. (*a*) Balance of the turbulent kinetic energy, $\frac{1}{2}\overline{q^2}$, equation. (*b*) Sketch showing the different zones of the plume based on the turbulent kinetic energy balance.

advection does not constitute as large a portion of this balance as it did for the temperature variance equation. After $\eta \approx 0.08$ the advection term changes its sign and becomes a loss to the budget. At the plume centre the gradient production term is about one-third of the advection and it increases until $\eta \approx 0.08$. Most of the contribution to this production comes from the shear stress term, $-\overline{uw}\,\partial W/\partial r$, except near the plume centre where $-\overline{w^2}\,\partial W/\partial z$ is dominant. The direct effect of buoyancy on turbulence is represented by the buoyancy production term and although it forms a substantial fraction of the balance, it is still about three times smaller than the gradient production. Therefore, most of the turbulence is maintained by the gradient production and not by the buoyancy. This is in contrast to the mean velocity field where the effect of buoyancy force was much more stronger.

The rate of mechanical dissipation ϵ was not measured and is obtained as the closing term in the balance. Like the temperature variance, the turbulent kinetic energy budget can also be divided into two regions. In the outer region ($\eta > 0.1$) the mechanisms of production and dissipation rate approximately balance each other and the flow can be considered in local equilibrium. In the inner region ($\eta < 0.1$) this is not true and the situation is qualitatively sketched in figure 14(*b*).

We can use the dissipation rate profile obtained above to calculate the turbulence Reynolds number $Re_T = ul/\nu = \overline{q^2}^2/9\epsilon\nu$. (Note that we have used the relations $\epsilon = u^3/l$ and $u^2 = \frac{1}{3}q^2$ in arriving at this definition.) The profile of this Reynolds number is shown in figure 15 for one representative height. The centreline value is about 1600.

It should be cautioned that at the outer edges of the plume ($\eta > 0.15$ or so) these balances are more qualitative than quantitative because of the hot-wire errors. This is especially true for the dissipation rates which are obtained as the closing terms in these balances because any errors present in the measurement of other quantities will be lumped into these. The largest error should be through the third-order moment (diffusion) terms. Since there are no errors involved in the temperature measurement,

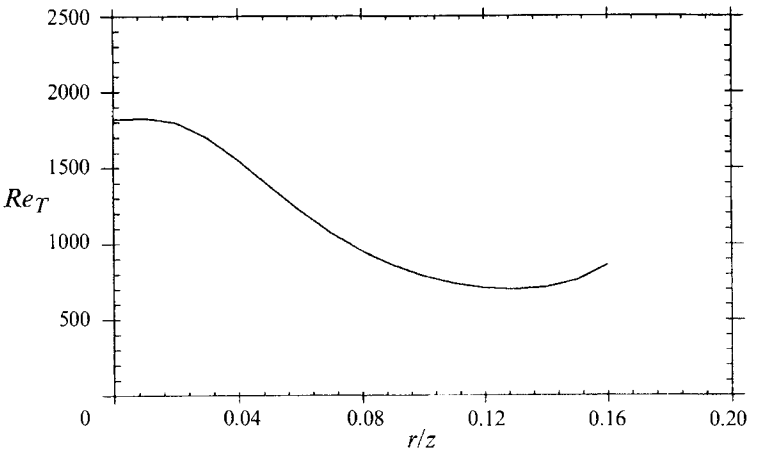

FIGURE 15. Profile of the turbulence Reynolds number across the plume at a vertical distance of $z/D = 15.7$.

the temperature variance balance is more accurate than the turbulent kinetic energy balance.

5. Further remarks and summary

This paper reports a comprehensive set of measurements in a fully developed round turbulent buoyant plume. The source and the boundary conditions of the flow were carefully measured and documented. The measurements of the ambient temperature ensured that the facility was not stratified and that the experiment corresponded to a plume in a neutral environment. Although a very simple and an easy aspect to measure, it is a very important part of the current experiment. The effect of stratification of the ambient fluid on the solutions admitted by the mean flow equations has been analysed for some time (see e.g. Batchelor 1954) but its importance in measurement of laboratory plumes in initially neutral environments was first realized by Beuther (1980). His study showed that plumes are quite sensitive to the changes in ambient fluid temperature and what might otherwise be considered a slight stratification can produce large changes in the mean flow. As was mentioned in §2.3, this influence of the ambient stratification enters the mean buoyancy equation through the $g\beta W \mathrm{d}T_\infty/\mathrm{d}z$ term and Beuther's (1980) study showed that under such conditions of stratification this term makes up a considerable fraction of the mean buoyancy budget. Since most of the experiments dealing with neutral environments do not monitor their ambient conditions, this has been suggested as one of the probable reasons for the differences in plume experiments (Beuther & George 1982). Another source of ambient disturbance is weak co-flowing streams which are set up in the ambient fluid in order to compensate for the entrained ambient fluid when experiments are conducted in relatively small water tanks (see George 1990). Appendix A details one case of this sensitivity which can occur when small circular screens are placed around the plume source. The findings of these studies and the experience in our laboratory shows that differences in the various plume experiments could be due more to the differences in their boundary conditions and due less to the differences in the instrumentation.

The present study confirmed some of the earlier measurements of mean flow variables. There are, however, large differences in the buoyancy field measurements of

the present study and that of Papanicolaou & List (1988). It should be noted that there are no hot-wire errors involved in the measurement of temperature. It should also be noted that the local total tracer flux in the experiments of Papanicolaou & List (1988) is much larger than its source value, rather than being equal to it (within certain experimental uncertainty). Papanicolaou & List (1988) argue that the reason for this was a systematic error in their mean concentration measurements and that when the mean temperature decay rates from their earlier investigation (Papanicolaou & List 1987) are employed then the total tracer flux is conserved. However, this line of argument is weak in the sense that it still does not prove that their experiment conserved tracer flux. On the other hand the present experiment conserves buoyancy flux within 10%.

It is very encouraging to note that the other studies which took care in ensuring that their facilities were not stratified and were free of any ambient disturbances obtained results which are very close to those reported here. For example the centreline values of mean buoyancy and velocity measured by Ogino *et al.* (1980) and the present values are exactly the same (they measured the centreline values only). The difference between the mean buoyancy profile measured here and that by Kotsovinos (1985) is only 6.5%. The present study used both a hot wire and thermocouples for the temperature measurement. The experiments of Ogino *et al.* (1980) and Kotsovinos (1985) employed thermocouples and thermistor probes respectively. These comparisons and facts give more credibility and confidence to the present measurements.

The balances of the mean buoyancy and momentum equation were also determined and the imbalance represents the error in the measurements. This is also the first time that such balances for a buoyant plume have been performed. The balance of the momentum equation clearly shows that the buoyancy force is as large as the transport by turbulent shear stress. This buoyancy force leads to larger velocity gradients in buoyant plumes than in jets and results in an increased production of turbulent energy through the gradient production term in the turbulent kinetic energy equation. This can be regarded as an indirect effect of buoyancy on turbulence.

The measurements allowed us to obtain balances of the temperature variance and turbulent kinetic energy. The thermal and mechanical dissipation rates were not measured and were obtained as the closing terms in these budgets. Despite certain measurements errors present in these budgets, which primarily emanate from the third-moment terms, they provide useful information about the relative importance of the different phenomenon. It is found that although the direct effect of buoyancy on the turbulent velocity field is substantial, most of the turbulence is still maintained by the gradient production. Therefore, it is concluded that in a buoyant plume the primary influence of buoyancy on turbulence is indirect, and enters through the mean velocity field (giving larger shear production). A contrast between the two budgets was the much larger magnitude of the advection of temperature variance as compared to the advection of turbulent kinetic energy.

It is cautioned that the moments involving velocity should be interpreted carefully toward the outer edges of the flow because of the larger hot-wire errors at these locations. This is especially true for the third moments. These moments and the temperature variance and turbulent kinetic energy budgets should be considered more qualitative than quantitative beyond $\eta \approx 0.15$. One possible way of avoiding these errors is to measure the flow with flying hot-wire probes such as used by Hussein *et al.* (1994) in their jet measurements. However, unlike jets, the velocities in laboratory plumes are very small in magnitude and a flight of probes through the flow will not only cause the plume to deflect or move off-centre, but will also introduce undesirable air

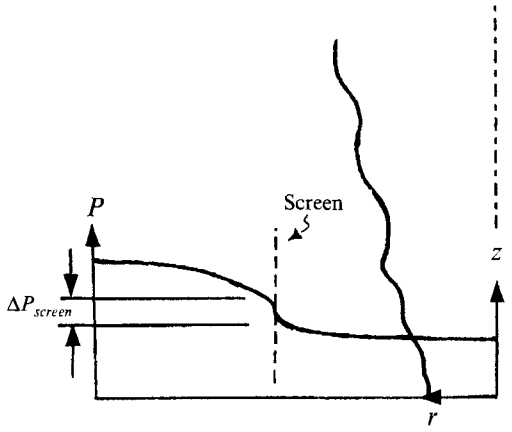

FIGURE 16. Sketch of the radial distribution of pressure near the plume source with a screen placed around its source.

currents in an otherwise quiescent environment. This will necessitate a long wait between probe traverses and will require a thorough probing of the facility for possible disturbances and stratification. The work in this direction is currently being evaluated by one of the authors (W.K.G.).

The authors are grateful to the referees whose careful review and thoughtful comments led to several improvements in the paper. An earlier version of this work was presented at the Turbulent Shear Flow Conference TSF 87. We are grateful to S. Woodward and M. Kotas for their contributions to this study, and to Professor D. B. Taulbee and to the late Professor C. B. Baker for their encouragement. This work was initiated with the support of NSF Atmospheric Science, Meteorology Program Grant No. ATM80-23699A01 and was completed with the assistance of NSF Engineering, Fluid Mechanics Program Grant No. MSM83-16833. The paper was finished while the first author was in residence at the Institute for Computational Mechanics in Propulsion, NASA Lewis Research Center.

Appendix A

The purpose of this appendix is to show the sensitivity of the boundary conditions on the growth of a laboratory plume. Our experience indicates that the differences in various experiments are mostly due to the differences in their boundary conditions rather than differences in their instrumentation. This sensitivity to the boundary conditions was studied by placing screens of different sizes around the plume source. These screens are employed in such experiments in an attempt to keep the cross-draughts and other such disturbances away from the flow. This is desirable because the velocities encountered in laboratory plumes are small ($\sim 1\ \mathrm{m\,s^{-1}}$) and because of this the flow can easily be affected by any small currents or disturbances present in the facility. These screens also help to keep the plume from meandering. It is always presumed that these screens do not influence the laboratory flow because these are usually placed well away from the edges of the flow and the measurements are taken at heights far above the source. In this appendix first we show that the screens influence the flow by modifying the inflow of surrounding fluid. Then mean flow measurements are presented to illustrate this effect.

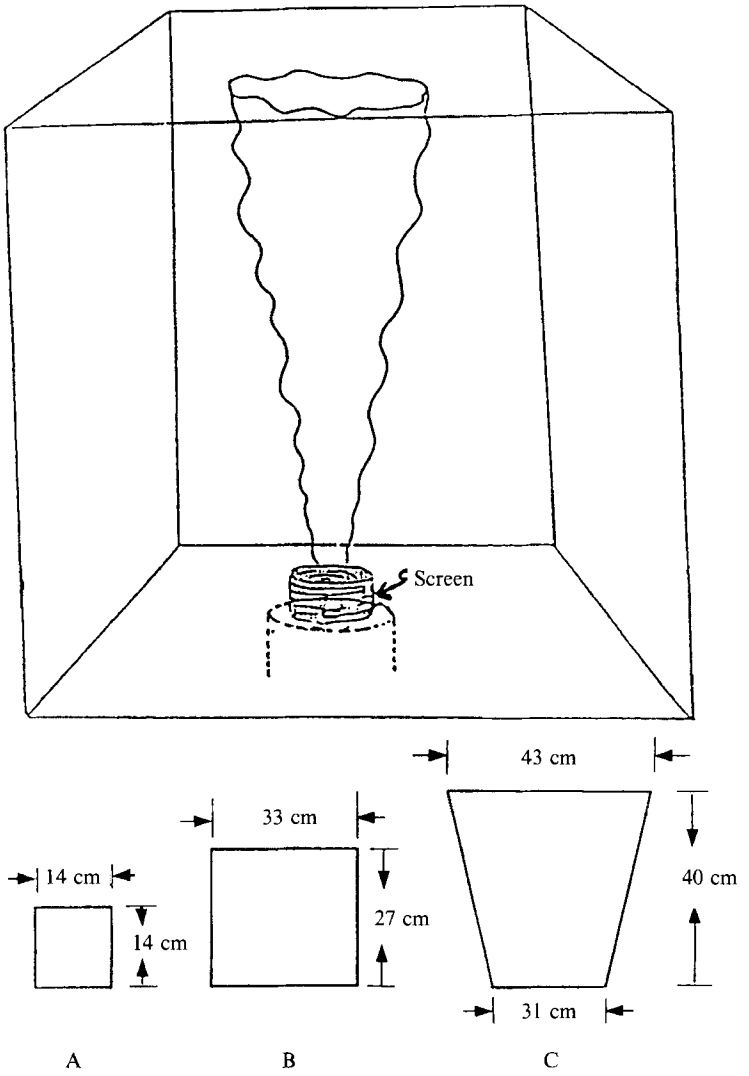

FIGURE 17. Sketch showing the placement of screens around the plume source and the size of the three screens used to study their effect on plume.

Keeping only the leading terms, the radial momentum equation for a round buoyant plume can be integrated from infinity to a given radius to obtain the equation for the mean pressure P (Tennekes & Lumley 1975)

$$P_\infty - P \approx \rho\overline{u^2}. \tag{A 1}$$

Therefore, the entrainment, which is driven by the above pressure difference, is of second order. Now consider a screen placed around the plume source as shown in figure 16. The effect of the screen is to reduce the pressure drop, thus reducing the inflow of the surrounding cooler air, i.e.

$$P_\infty - P \approx \rho\overline{u^2} + \Delta P_{screen}. \tag{A 2}$$

If the screen is modelled by a simple pressure coefficient, then

$$P_\infty - P \approx \rho\overline{u^2} + \tfrac{1}{2}K\rho U_s^2, \tag{A 3}$$

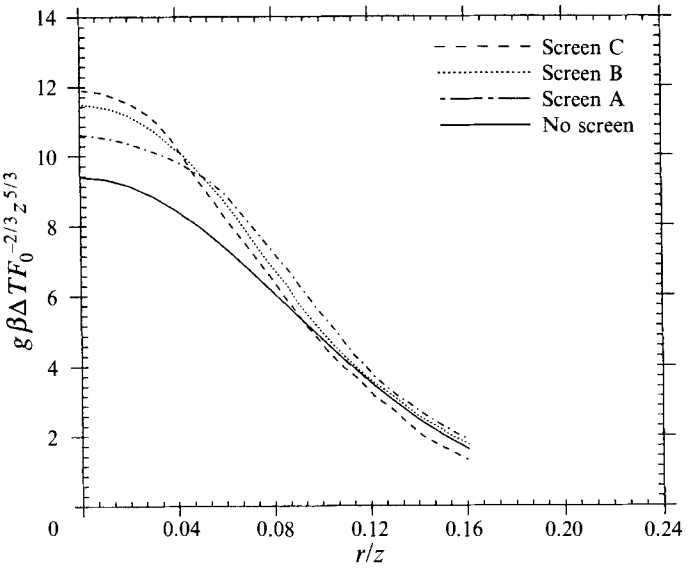

FIGURE 18. The mean buoyancy profiles (measured with thermocouples) corresponding to the three different screens placed around the plume source. For comparison the buoyancy profile measured without a screen placed around the plume source is also shown. The data are plotted in similarity variables.

where K is the screen constant and U_s is the entrainment velocity at the location where the screen is placed. From (A 3) we see that the screen will leave the entrainment field unchanged only if

$$\tfrac{1}{2}K\rho U_s^2 \ll \rho\overline{u^2}. \tag{A 4}$$

For round geometry this can always be satisfied by placing the screens far enough away since $U \to 1/r$ as $r \to \infty$. (Note that the measurements to be presented next do not correspond to such a case.)

To support the above analysis mean buoyancy profiles were measured, using thermocouples, with three different size screens placed around the plume source (see figure 17). Figure 18 shows the mean buoyancy profiles corresponding to these screens along with the profile measured without using any screen. We note that the effect of the screens is to make the buoyancy profiles narrower and higher. This is because the screens reduce the inflow of the surrounding cooler air into the main flow as was suggested by the above.

More detailed hot-wire measurements were carried out for screen C in order to document the screen effects on mean as well as turbulence quantities. Only the mean flow quantities are given here. (Turbulence quantities are given in Shabbir & George 1992.) These measurements were carried out using the two-wire probe which is described in §3.2. The results are presented in figures 19(*a*) and 19(*b*). We note that the data collapse is excellent (and even better than the measurements presented in the main paper). The measurements satisfy the integral buoyancy constraint given by equation (12) (these results are given in Shabbir 1987). This shows that the collapse of experimental data into similarity variables and conservation of buoyancy (or any other relevant integral constraint) does not necessarily mean that the experiment represents the flow which one set out to measure. One must check the facility carefully to make sure that no external influences are present.

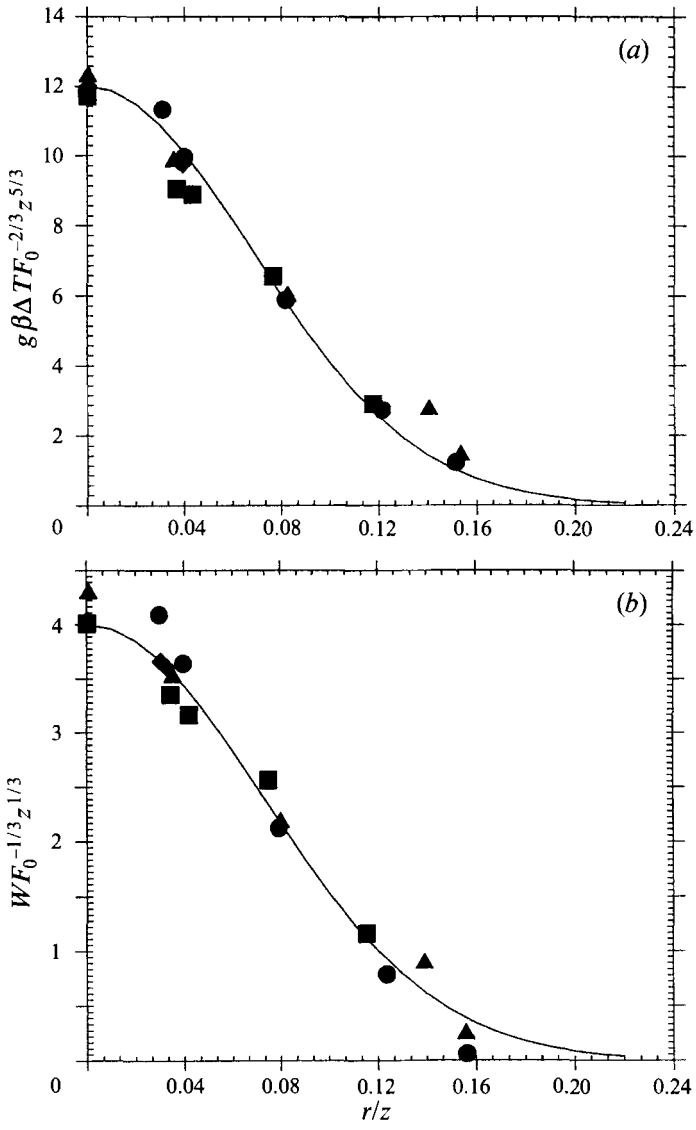

FIGURE 19. (*a*) Mean buoyancy profile and (*b*) mean vertical velocity profile measured with a hot-wire probe with the screen C placed around the plume source. ●, $z/D = 15$; ▲, $z/D = 17$; ■, $z/D = 19$; ◆, $z/D = 21$. The data are plotted in similarity variables.

The above analysis can be extended to cases where the boundary conditions of the experiment involve weak co-flowing streams etc. since these also modify the entrainment flow. This is discussed in detail in a review paper by George (1990).

Appendix B

This appendix gives the polynomial fits to the data. Lists of the experimental data which are plotted in various figures of the paper are available from the authors or JFM Editorial Office. Note that all the data are given in similarity variables and can easily be converted into dimensional form by using the appropriate vertical distance and the source buoyancy flux given in table 1.

In performing the curve fits the two-wire-probe measurements (if available) were preferred over the three-wire-probe measurements. As was pointed out in §4.4, some of the moments have small non-zero values at the plume centre rather than being zero (e.g. shear stress in figure 7*d*). However, for curve-fitting purposes all such moments were assigned a zero value at the plume centre. Owing to large scatter in some of the moments, their curve fits are at best an approximation.

The polynomial fits to the experimental data are as follows:

$$\overline{w^2}F_0^{-2/3}z^{2/3} = \frac{1.1+200\eta^2}{(1+38\eta^2)^4}, \quad \overline{u^2}F_0^{-2/3}z^{2/3} = \frac{0.65+67.35\eta^2-227.26\eta^4}{(1+30\eta^2)^4},$$

$$\overline{uw}F_0^{-2/3}z^{2/3} = \frac{6.5\eta-104.23\eta^3}{(1+24\eta^2)^3}, \quad g^2\beta^2\overline{t^2}F_0^{-4/3}z^{10/3} = \frac{12.5+2009.1\eta^2}{(1+30\eta^2)^6},$$

$$g\beta\overline{wt}F_0^{-1}z^2 = \frac{1.85+680\eta^2}{(1+32\eta^2)^6}, \quad g\beta\overline{ut}F_0^{-1}z^2 = \frac{23\eta}{(1+41\eta^2)^3},$$

$$\overline{w^3}F_0^{-1}z = \frac{0.38+10.6\eta^2+21\,593.6\eta^4-371\,355\eta^6}{(1+27\eta^2)^6}, \quad \overline{u^3}F_0^{-1}z = \frac{2.4\eta+157\eta^3}{(1+27\eta^2)^6},$$

$$\overline{uw^2}F_0^{-1}z = \frac{-4.6\eta+2035.3\eta^3-12430.9\eta^4+17881.0\eta^5}{(1+27\eta^2)^6},$$

$$\overline{u^2w}F_0^{-1}z = \frac{-0.07-26.94\eta^2+2429.21\eta^3-15618.29\eta^4+193866.46\eta^6}{(1+27\eta^2)^6},$$

$$g\beta\overline{w^2t}F_0^{-4/3}z^{7/3} = \frac{0.75+226\eta^2+11\,740\eta^4}{(1+26\eta^2)^6},$$

$$g^2\beta^2\overline{wt^2}F_0^{-5/3}z^{11/3} = \frac{2.9+746.3\eta^2-4309.35\eta^6}{(1+23\eta^2)^6},$$

$$g^2\beta^2\overline{ut^2}F_0^{-5/3}z^{11/3} = \frac{8381.55\eta^3-35932.23\eta^4+98082.8\eta^6}{(1+27\eta^2)^6}.$$

REFERENCES

BAKER, C. B., TAULBEE, D. B. & GEORGE, W. K. 1980 An analysis of buoyant jet heat transfer. *Proc. 7th Heat Transfer Conf., Munich.*

BATCHELOR, G. K. 1954 Heat convection and buoyancy effects on fluids. *Q. J. R. Met. Soc.* **80**, 339–358.

BEUTHER, P. D. 1980 An experimental investigation of the turbulent buoyant plume. PhD Dissertation, SUNY at Buffalo, Buffalo, NY.

BEUTHER, P. D. & GEORGE, W. K. 1982 The turbulent buoyant plume in a stratified environment. *Proc. Natl Congr. Theor. and Appl. Mech.*, Cornell University, Ithaca, NY.

CHEN, C. J. & RODI, W. 1980 *Vertical Turbulent Buoyant Jets.* Pergamon.

GEORGE, W. K. 1990 Governing equations, experiments, and the experimentalist. *Exp. Thermal Fluid Sci.* **3**, 557–566.

GEORGE, W. K., JR., ALPERT, R. L. & TAMANINI, F. 1977 Turbulence measurements in an axisymmetric buoyant plume. *Intl J. Heat Mass Transfer* **20**, 1145–1154.

GEORGE, W. K., BEUTHER, P. D. & SHABBIR, A. 1989 Polynomial calibrations for hot wires in thermally-varying flows. *Exp. Thermal Fluid Sci.* **2**, 230–235.

HUSSEIN, H. J., CAPP, S. P. & GEORGE, W. K. 1994 Velocity measurements in a high Reynolds number momentum-conserving axisymmetric turbulent jet. *J. Fluid Mech.* **258**, 31–75.

KOTSOVINOS, N. E. 1985 Temperature measurements in a turbulent round plume. *Intl J. Heat Mass Transfer* **28**, 771–777.

KOTSOVINOS, N. E. & LIST, E. J. 1977 Turbulent buoyant jets. Part 1. Integral properties. *J. Fluid Mech.* **81**, 25–44.

LIST, E. J. 1982 Turbulent jets and plumes. *Ann. Rev. Fluid Mech.* **114**, 189–212.

LIST, E. J. & IMBERGER, J. 1973 Turbulent entrainment in buoyant jets and plumes. *Proc. ASCE, J. Hydraul. Div.* **99**, 1416–1474.

LUMLEY, J. L. 1971 Explanation of thermal plume growth rates. *Phys. Fluids* **14**, 2537–2538.

LUMLEY, J. L. 1978 Computational modeling of turbulent flows. *Adv. Appl. Mech.* **18**, 123–176.

MORTON, B. R. 1959 Forced plumes. *J. Fluid Mech.* **2**, 151–163.

MORTON, B. R., TAYLOR, G. I. & TURNER, J. S. 1956 Turbulent gravitational correction from maintained and instantaneous sources. *Proc. R. Soc. Lond.* A **234**, 1–23.

NAKAGOME, H. & HIRATA, M. 1977 The structure of turbulent diffusion in an axisymmetrical thermal plume. In *Proc. 1976 ICHMT Seminar on Turbulent Buoyant Convection*, pp. 361–372. Hemisphere.

OGINO, F., TAKEUCHI, H., KUDO, I. & MIZUSHINA, T. 1980 Heated jets discharged vertically into ambients of uniform and linear temperatures profiles. *Intl J. Heat Mass Transfer* **23**, 1581–1588.

PAPANICOLAOU, P. N. & LIST, E. J. 1987 Statistical and spectral properties of tracer concentration in round buoyant jets. *Intl J. Heat Mass Transfer* **30**, 2059–2071.

PAPANICOLAOU, P. N. & LIST, E. J. 1988 Investigations of round vertical turbulent buoyant jets. *J. Fluid Mech.* **195**, 341–391.

PAPANTONIOU, D. & LIST, E. J. 1989 Large scale structure in the far field buoyant jets. *J. Fluid Mech.* **209**, 151–190.

RODI, W. 1986 Vertical turbulent buoyant jets: experimental findings and prediction methods. *Proc. Intl Symp. on Buoyant Flows, Athens, Greece, Sept. 1–5.*

ROUSE, J., YIH, C. S. & HUMPHREY, H. W. 1952 Gravitational convection from a boundary source. *Tellus* **4**, 201.

SCHMIDT, W. 1941 Turbulent propagation of a stream of air. *Z. Angew. Math. Mech.* **21**, 265–278.

SHABBIR, A. 1987 An experimental study of axisymmetric turbulent buoyant plume and investigation of closure hypotheses. PhD dissertation, SUNY at Buffalo, Buffalo, NY.

SHABBIR, A., BEUTHER, P. B. & GEORGE, W. K. 1994 X-wire response in turbulent flows of high intensity turbulence and low mean velocities. *Exp. Thermal Fluid Sci.* (submitted).

SHABBIR, A. & GEORGE, W. K. 1985 Measurements of temperature and velocity in an axisymmetric turbulent buoyant plume. *Bull. Am. Phys. Soc.* **30**, 10, Abstract DD6.

SHABBIR, A. & GEORGE, W. K. 1987 An experimental study of an axisymmetric turbulent buoyant plume in a neutral environment. *Proc. 6th Turbulent Shear Flow Conf., Toulouse*, pp. 9-3-1–9-3-6.

SHABBIR, A. & GEORGE, W. K. 1992 Experiments on a round turbulent buoyant plume. *NASA TM* 105955.

TENNEKES, H. & LUMLEY, J. L. 1972 *A First Course in Turbulence*. MIT Press.

TOWNSEND, A. A. 1956 *Structure of Turbulent Shear Flows*. Cambridge University Press.

TUTU, N. K. & CHEVRAY, R. 1975 Cross-wire anemometry in high intensity turbulence. *J. Fluid Mech.* **71**, 785–800.

ZEL'DOVICH, YA. B. 1937 Limiting laws for turbulent flows in free convection. *Zh. Eksp. Theoret. Fiz* **7**, 1463.